Covalent and non-covalent systems based on s-, p-, and d-metal macroheterocyclic complexes and fullerenes

N. G. Bichan★ and E. N. Ovchenkova

G. A. Krestov Institute of Solution Chemistry, Russian Academy of Sciences, 1 ul. Akademicheskaya, 153045 Ivanovo, Russian Federation. Fax: +7 (493 2) 33 6265. E-mail: bng@isc-ras.ru

The review summarizes various systems containing macroheterocyclic donor platforms and fullerenes. The specific features of the chemical structure and spectral properties of such molecular systems, charge transfer processes in complexes and mechanisms of their formation, and potential fields of their practical application are considered. Special attention is given to supramolecular systems, in which metal-containing porphyrins/phthalocyanines bearing a complex-forming cation other than zinc act as electron donors.

Key words: porphyrins, phthalocyanines, macroheterocyclic complexes, fullerenes, conjugate, supramolecular system, photoinduced charge transfer, spectral properties.

Introduction

Molecular systems based on a donor and an acceptor have attracted attention due to their ability to undergo photoinduced charge separation. This fundamental process is essential for both the natural photosynthesis and solar energy conversion.[1] In the past decades, supramolecular assemblies, which can be considered as models of natural photosynthetic systems, have been extensively investigated.[2—4] Porphyrins (Porph), phthalocyanines (Pc) as their analogs, and complexes based on them have long been recognized as excellent electron donors. Fullerenes, in turn, display electron-acceptor properties and exhibit fast charge separation, which is one of parameters required for ideal photosynthetic model systems.[5] There are several approaches to the chemical design of systems based on macroheterocyclic donor platforms and fullerenes: the synthesis of complexes with rigid and relatively flexible covalent linkers and the preparation of non-covalent supramolecular systems. The synthesis and characterization of covalently linked porphyrin—fullerene complexes were important for an understanding of the mechanism of regulation of photoinduced electron transfer in molecular systems.[6—8] However, supramolecular artificial photosynthetic systems stabilized by non-covalent bonds, such as hydrogen bonds, anionic and crown ether—ammonium interactions, metal—ligand coordination, and electrostatic interactions, are more promising.[9] Most publications are devoted to the synthesis of such systems based on zinc porphyrinates/phthalocyaninates and fullerenes;[10—14] however, porphyrin/phthalocyanine complexes of other s-, p-, and d-metals, such as magnesium,[15,16] copper,[17,18] aluminum,[19—21] tin,[22—24] indium,[25,26] cobalt,[27—34] manganese,[34,35] iron,[17,34,36] molybdenum,[37—39] rhenium,[40,41] ruthenium,[42,43] *etc.*, are considered in order to expand the potential of the design of photoactive systems. Systems based on paramagnetic metal porphyrinates/phthalocyaninates and fullerenes can be used as single-molecule magnets (SMM).[44] It is worth noting that some metals (cobalt, molybdenum, ruthenium) have high coordination capacity in the synthesis of supramolecular complexes of different compositions (1 : 1, 2 : 1).[28,42] The ability of aluminum and tin to form Porph/Pc complexes with hydroxy ligands allows the synthesis of covalently linked fullerene-containing axial complexes.[19,22] The incorporation of biologically active metals, *e.g.*, cobalt or manganese, into the cavity of the macrocycle makes such molecular systems promising antibacterial/antifungal agents[45—47] and artificial enzymes.[48] In this review, the results of the synthesis of fullerene-containing systems based on s-, p-, and d-metal porphyrin/phthalocyanine complexes are summarized and analyzed. The specific features of the chemical structures and spectral properties of these molecular systems are considered. The charge transfer processes in complexes, the mechanisms of their formation, and potential fields of their practical application are discussed.

1. Synthesis of covalent systems based on s-, p-, and d-metal macroheterocyclic complexes and fullerenes

Systems with rigid covalent linkers are important for an understanding of the mechanism of photoinduced electron transfer, because they are characterized by the exact mutual orientation of the donor and acceptor.[8] In one of the pioneering studies,[2] the authors synthesized

Published in Russian in *Izvestiya Akademii Nauk. Seriya Khimicheskaya,* No. 2, pp. 239—275, February, 2021.

Scheme 1

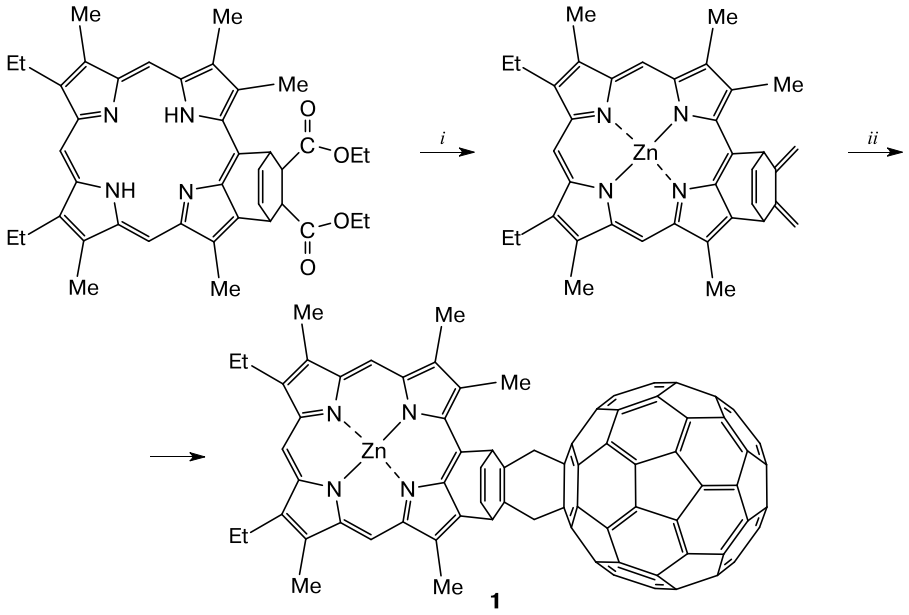

i. 1) $LiAlH_4$, 2) $MeSO_2Cl$, 3) $Zn(OAc)_2$, 4) $KOCMe_3$. *ii*. C_{60}, PhMe.

a dyad, in which the chromophore is linked to fullerene C_{60} by a bicyclic bridge, and studied their photochemical characteristics. Conjugate **1** was synthesized in 34% yield by the Diels—Alder reaction according to Scheme 1. The electronic absorption spectrum (UV-Vis) of dyad **1** shows absorption bands of metalloporphyrin (M(Porph)) and fullerene at 325, 425, 550, and 590 nm. However, the Soret band and *Q* bands were bathochromically shifted by 9—12 nm with respect to the corresponding bands of free M(Porph). The investigation of the electron transfer in dyads by time-resolved fluorescence and transient absorption spectroscopy showed that the lifetime of the excited state of conjugate **1** was 5 ps, and the charge-separated state $[Zn(Porph)]^{\bullet+}$—$C_{60}^{\bullet-}$ can occur both in polar and nonpolar solvents (benzonitrile and toluene). Therefore, these compounds are of interest as photosynthetic systems in the field of solar energy conversion and molecular optoelectronics, which facilitates the development of synthetic aspects.

Different approaches to the synthesis of covalently linked dyads based on Porph and fullerene C_{60} are reported in the literature.[49—52] For instance, Boyd and co-workers[49,50] synthesized conjugate **2** from β-formyltetraphenylporphyrin using the Prato reaction for the functionalization of fullerenes.[53] The UV-Vis spectrum of compound **2** shows maxima at 430, 555, and 592 nm, which are bathochromically shifted by 5 nm with respect to the model zinc porphyrinate methyl-substituted at the β position. The intensity of the fluorescence spectrum of this dyad in toluene is much lower than that of the corresponding metalloporphyrin. The spectrum of the model zinc complex has emission maxima at 599 and 648 nm and the quantum yield of 0.03, whereas these maxima for dyad **2** appear at 722 and 803 nm and correspond to the emission of the fullerene entity with a quantum yield of 0.0003. No intense bands of the porphyrin component of conjugate **2** were observed in the spectrum. The lifetime of the charge-separated system was 50 ps.

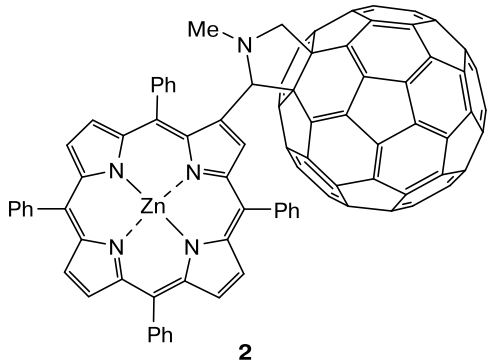

Porphyrin—fullerene dyads with different spacers (**3—6**) were synthesized by the Diels—Alder reaction using the donor—spacer—acceptor architecture.[51,52] It should be noted that the β positions of the macrocycle in these dyads, like those in dyad **2**, are not involved in this process.

The three-band UV-Vis spectra of these systems in THF consist of an intense Soret band (from 425 to 431 nm) and *Q* bands at 557—599 nm and are almost identical to the UV-Vis spectra of the corresponding zinc porphyrinates. The largest changes are observed in the UV-Vis spectrum of the system containing spacer **5**, which shows

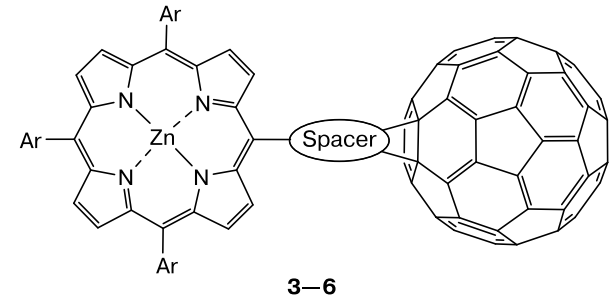

3—6

Ar = 3,5-$Bu^t_2C_6H_3$

Spacers:

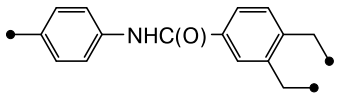

(**3**),

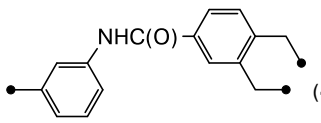

(**4**),

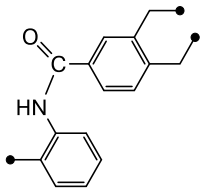

(**5**),

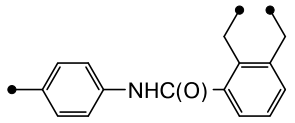

(**6**)

the bathochromic shift of the Soret band by 6 nm relative to that of the corresponding zinc(II) porphyrinate. Besides, the intensity of the Soret band decreases, which is apparently associated with the arrangement of the porphyrin and the fullerene entities and their interaction in the conjugate due to specific features of the spacer chemical structure. The fluorescence spectra of all systems recorded in THF and benzene display fluorescence quenching with respect to the corresponding Porph. Since the fluorescence spectrum of conjugate **4** in THF shows bands corresponding not only to porphyrin but also to the fullerene moiety of the molecule, the authors noted that the occurrence of the energy transfer in the conjugate cannot be evaluated from the spectra. These comparative studies clearly demonstrate the effect of the chemical structure on the charge transfer process. The time-resolved transient absorption spectroscopy measurements showed that the photoinduced charge separation (CS) and charge recombination (CR) occur in all Porph—C_{60} systems regardless of the bond between the chromophores. The chemical structure of the spacer influences the rate of the CS and CR processes; the lowest values were found for the *meta* isomer.

Chlorin—fullerene conjugates were synthesized using the reactions of alkenes with acetylenes to form 1,3-dienes (so-called enyne metathesis) and the Diels—Alder reaction.[54] These conjugates showed significant fluorescence quenching compared to chlorin and its complex with zinc. Later, fullerene-containing *N*-hexylpurpurinimide conjugates were synthesized[55] by the introduction of the fullerene at different positions and were used in photoinduced electron transfer studies.[56] Investigations performed in a wide temperature range from −150 to 65 °C demonstrated that conjugate **7** contains the closely spaced donor and acceptor and has a long lifetime of the charge-separated state.[56] At −150 °C, conjugate **7** has an ultra-long lifetime (120 s). Hence, fullerene-containing conjugates can be considered as photosensitizers with a long-lived charge-separated state.[57]

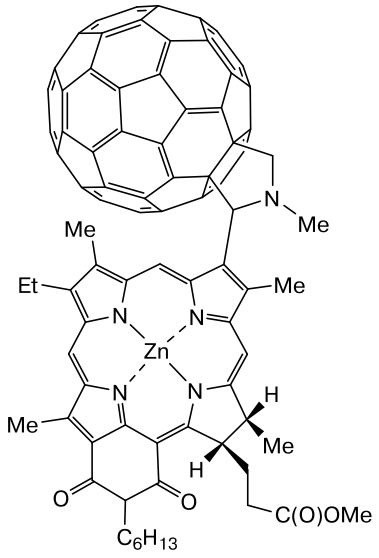

7

Comparative studies aimed at elucidating the structure—property relationships are an important step in the design of systems capable of converting solar energy. Methods for the preparation of various Porph—C_{60} conjugates are considered in the review.[58] Various approaches to the accomplishment of these processes are reported in the publications.[59—67] There are several strategies for the design of covalently linked porphyrin—fullerene systems, which make it possible to improve their physicochemical characteristics: the variation of the spacer structure,[52,63] the variation of the macrocycle periphery,[64,65,68] the inclusion of additional donor or acceptor groups in the conjugates[69] (*e.g.*, Porph dimers as donor platforms[61]), and the use of different metals as the central cation in the macrocycle.

In the fluorescence spectra of first triazole-bridged Porph—C_{60} dyads **8** and **9** in THF and toluene, efficient fluorescence quenching was observed compared to the corresponding porphyrins, which is indicative of a strong binding between the donor and acceptor and the efficient photoinduced electron transfer.[63]

For zinc phthalocyaninate (ZnPc)—fullerene conjugate **10** connected by a long flexible spacer, the lifetime of the charge-separated state was 7.4 ps, and the charge recombination time in chlorobenzene was 2.2 ns. Dyads

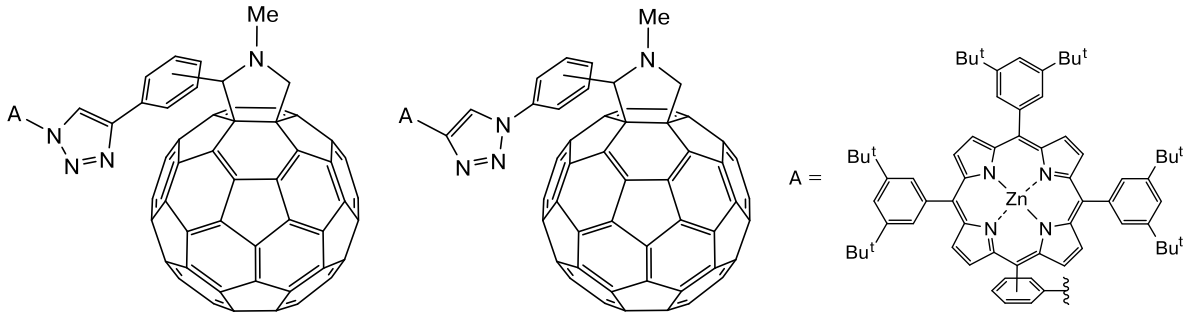

8 **9**

containing shorter flexible bridges have longer lifetimes (from 32 ps to 10 ns) for radical ion pairs depending on the solvent nature.[71]

The photoinduced electron transfer in liquid-crystalline ZnPc—C_{60} conjugates was first reported in the study.[70] The UV-Vis spectrum of system **10** in THF shows bands characteristic of the corresponding zinc phthalocyaninate: a Soret band at 350 nm and an intense *Q* band at 679 nm with a shoulder at 612 nm. In the fluorescence spectrum, the intensity of the band at 684 nm assigned to zinc phthalocyaninate in the conjugate is significantly decays compared to free ZnPc; the quantum yields are 0.05 and 0.33, respectively. The photoinduced electron transfer in conjugate **10** was studied by time-resolved transient absorption spectroscopy, and the rate constants for the charge separation (k_{CS}) and charge recombination (k_{CR}) in toluene were evaluated to be $5.5 \cdot 10^9$ and $5.2 \cdot 10^8$ s^{-1}, respectively.

Not only the spacer nature but also the macrocycle periphery can influence the physicochemical characteristics of the Pc—C_{60} systems. The evaluation of the effect of substituents of different nature at the phthalocyanine ring on the photoinduced electron transfer in these systems demonstrated that the introduction of fluorine-containing substituents can interrupt this process in dyad **11**. This fact

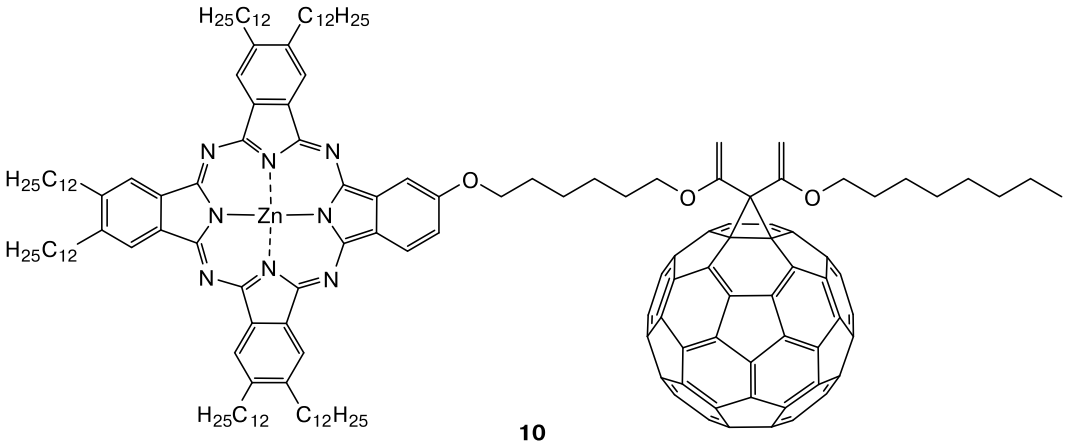

10

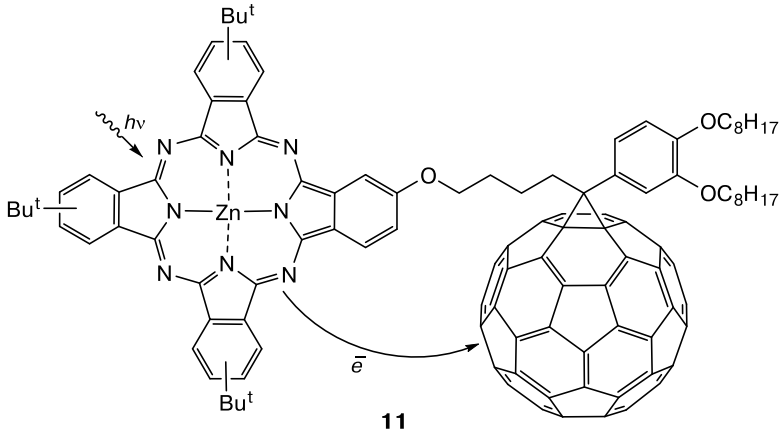

11

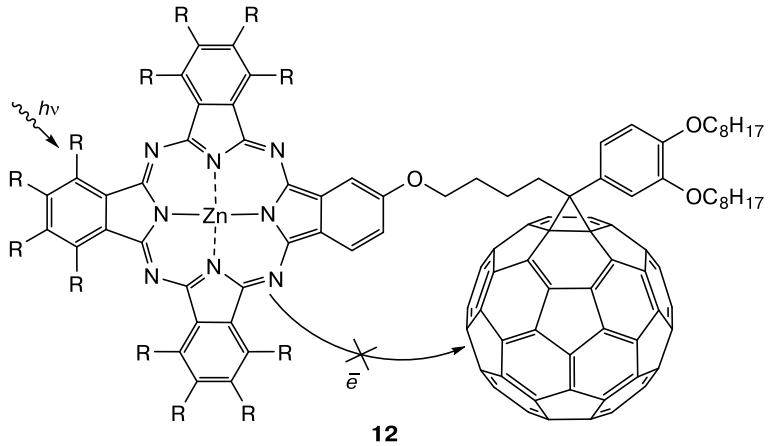

12

was attributed[64] to the strong electron-withdrawing nature of trifluoroethoxy groups, resulting in equivalent electron-acceptor properties of phthalocyanine and C_{60}.

The introduction of substituents into the macrocycle or on the fullerene cage to acquire water solubility opens the opportunity to use the conjugates for biological purposes. Kotel´nikov *et al.*[72] demonstrated the possibility of the formation of a system based on sulfonated aluminum phthalocyaninate (AlPcS) and the polycationic fullerene C_{60} derivative (PFD). The addition of PFD to a solution of AlPcS causes a decrease in the intensity of the fluorescence decay kinetic curves (by more than two orders of magnitude) with no changes in the decay time, which is indicative of the formation of a steady-state complex. The results of spectroscopic studies provide evidence for the excitation (or electron) transfer to the fullerene cage in this complex, which facilitates enhanced singlet oxygen generation. It was shown that the complex of the photosensitizer with PFD exhibits photodynamic activity, which is higher than the activity of the individual components by a factor of 20 and 108 for AlPcS and PFD, respectively.

The investigation of photophysical and photochemical properties of water-soluble complexes based on chlorin e_6 and fullerene derivatives[73] is of certain interest. Thus, the zinc chlorin e_6 complex—polyanionic fullerene conjugates showed a 70-fold fluorescence quenching compared to the fullerene-free complex. The fluorescence lifetime of this conjugate was <0.4 ns. Photophysical measurements provided evidence that the photodynamic mechanism of singlet oxygen generation can be switched to the superoxide generation in dyads. However, after the inclusion of the central Zn^{2+} cation into the chlorin e_6 molecule, the photodynamic activity and phototoxicity of this dyad become insignificant despite the long-lived charge-separated state. The interaction of these dyads with liposomal membranes leads to a sharp increase in the fluorescence signal. All these aspects are attractive not only for the design of efficient photosensitizers but also as a platform for the construction of different systems for the switching-off at the nanolevel.

Metal-complexing agents other than zinc also have attracted attention in order to extend the potential of the design and expand the range of application of these macroheterocyclic complexes with fullerenes.

Magnesium is present in chlorophyll,[75] which is directly involved in the photosynthesis. Hence, the incorporation of magnesium macroheterocyclic complexes into donor-acceptor conjugates, required for the design of artificial photosynthetic systems, is a challenging problem.

Conjugate **13** based on magnesium porphyrinate and fullerene was synthesized from the corresponding Porph—C_{60} and $MgBr_2 \cdot OEt_2$ in triethylamine within 30 min (78% yield) and studied by spectroscopic, electrochemical, and photophysical methods.[76] The visible region of the UV-Vis spectrum of dyad **13** corresponds to the UV-Vis spectrum of magnesium tetraphenylporphyrinate (MgTPP); the band at 330 nm characteristic of fullerene is observed in the UV region. The UV-Vis spectra of many Porph/Pc—C_{60} dyads are the overall spectra of their components.

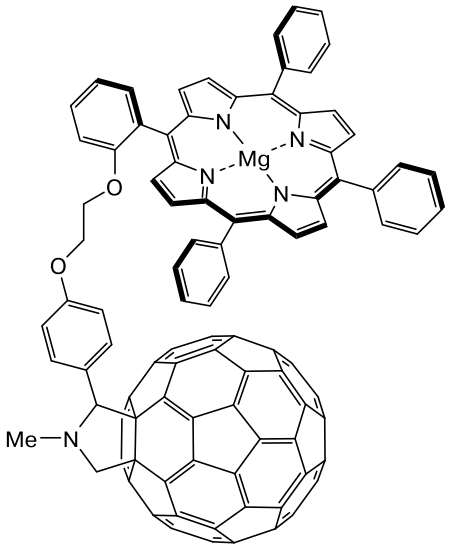

13

Table 1. Rate constants for the charge separation (k_{CS}) and charge recombination (k_{CR}) in magnesium and zinc tetraphenylporphyrinates (MgTPP and ZnTPP, respectively) conjugated to fullerene[76]

Dyad	Solvent	k_{CS}/s^{-1}	$\Phi_{CS}{}^{C}$	$k_{CR/s}{}^{-1}$	τ_{RIP}/ns
MgTPP—C_{60} **13**	DMF	$1.7 \cdot 10^9$	0.69	$3.3 \cdot 10^6$	300
	Dichlorobenzene	$9.5 \cdot 10^8$	0.55	$1.9 \cdot 10^6$	510
	Toluene	$7.0 \cdot 10^8$	0.47	$1.8 \cdot 10^8$	<10
ZnTPP—C_{60}	DMF	$2.2 \cdot 10^9$	0.74	—	—
	Dichlorobenzene	$1.5 \cdot 10^9$	0.67	$5.9 \cdot 10^7$	20
	Toluene	$8.5 \cdot 10^8$	0.54	—	—

Note. $\Phi_{CS}{}^{C}$ is the quantum yield of the charge-separated state of the fullerene component of the dyad, τ_{RIP} is the lifetime of the radical ion pair.

However, at high concentrations of the conjugates, a new broad band appears in the region of 750—1000 nm assigned to the interaction between the porphyrin and fullerene components of the dyad in the ground state. The results of the study of the electron transfer in system **13** by time-resolved fluorescence (k_{CS}) and transient absorption spectroscopy (k_{CR}) are given in Table 1.

A comparative analysis of dyad **13** with the related zinc complex[77] indicates the better charge stabilization in the magnesium complex. Hence, magnesium porphyrins are promising candidates for the synthesis of covalently linked Porph—C_{60} dyads capable of efficient photoinduced electron transfer.

Conjugate **14** composed of two complexes based on substituted magnesium tetraphenylporphyrinate and fullerene was synthesized in the study.[16] Scheme 2 shows a schematic representation of the light-to-photocurrent conversion system for conjugate **14** deposited onto an ITO

Scheme 2

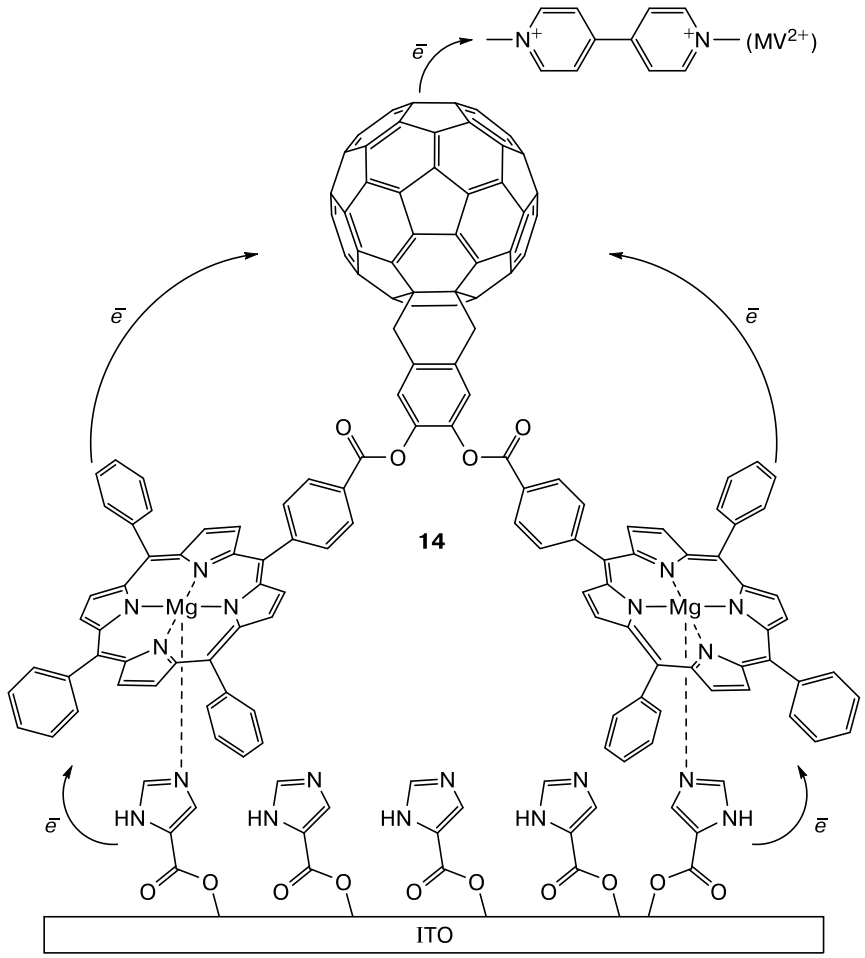

(indium tin oxide) substrate. The quantum yield of the photocurrent conversion system with conjugate **14** based on magnesium porphyrinate was 7.8%, whereas the quantum yield for the corresponding system with zinc porphyrinate was 0.64%, and that for fullerene-free ZnPorph was 0.043%. Hence, it was concluded that the longer the lifetime of the excited singlet state and the more efficient the charge separation, the better performance of the solar energy conversion system.

In the construction of covalently linked fullerene-containing conjugates, attention is given to aluminum and tin porphyrinates/phthalocyaninates as donor platforms. In these conjugates, the macrocycle is generally linked to fullerene by axial covalent bonds through oxygen. This arrangement of the donor and acceptor provides an efficient overlap of their orbitals similar to a natural photosynthetic system, in which an axially bound amino acid is involved in the electron transfer.[78] Taking into account the oxophilicity of these metals, aluminum and tin macroheterocyclic complexes are used to prepare functionally active axial-bonding-type molecular arrays.[79]

Systems based on aluminum(III) porphyrinate, substituted fullerene containing the carboxy group, and ferrocene were characterized in the study.[20] Dyad **15** was synthesized by the condensation of metalloporphyrin and substituted fullerene. The synthesis of triad **16** involves the following three steps: the attachment of ferrocene to the porphyrin macrocycle through an amide bond, the preparation of the aluminum(III) porphyrin complex, and the formation of the final porphyrin—fullerene conjugate. The products were obtained in yields higher than 90%.

The UV-Vis spectrum of the conjugates is a superposition of the UV-Vis spectra of the individual chromophores — an intense Soret band (416 nm), a *Q* band (547 nm), and absorption bands of the fullerene entity at 256 and 700 nm. In the UV-Vis spectrum of triad **16**, the band characteristic of absorption of ferrocene was masked by more intense components. A comparison of the fluorescence intensity with that of the reference compound (aluminum porphyrinate) showed a significant decay, which was most intense in the case of triad **16**. The charge separation rate constants k_{CR} are $2.54 \cdot 10^7$ and $5.70 \cdot 10^7$ s^{-1} for dyad **15** and triad **16**, respectively. The lifetime of the radical ion pair is 39 ns, which is 2.3 times longer compared to dyad **15**. Photoelectrochemical studies of OTE/SnO_2 electrodes (OTE is an optically transparent electrode) modified with the synthesized compounds demonstrated that use of ferrocene as the secondary electron donor is unfavorable. The photocurrent spectrum showed that the maximum incident photon-to-current efficiency (IPCE) for the AlPorph—C_{60} conjugate is 23 and 21% at 450 and 550 nm, respectively. The introduction of ferrocene into this conjugate leads to a decrease in the maximum values of IPCE to 20% at 430 nm and 14% at 560 nm.

The influence of secondary donors of different nature on the electron and energy transfer processes in systems

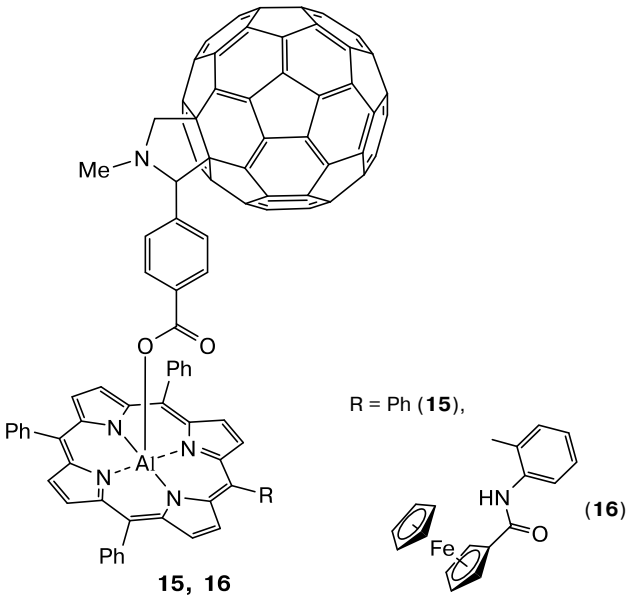

15, 16

based on aluminum(III) porphyrinates and fullerenes was addressed in several studies.[21,80,81] The introduction of phenothiazine and 2-methylphenothiazine[80] into covalently linked aluminum(III) porphyrinate—fullerene conjugates (**17**) promotes an approximately twofold increase in τ_{RIP} with respect to the lifetime of systems **15**, in which

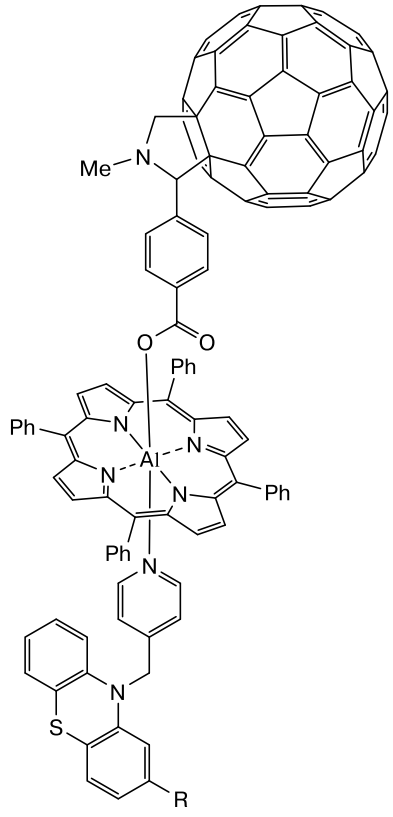

17

R = H, SCH_3

the secondary donor is absent, and a five-fold increase compared to ferrocene-containing triad **16**,[20] which provides an additional path to rapid recombination of the radical ion pair.

A series of conjugates based on aluminum(III) porphyrinate, tetrathiafulvalenes (TTF), and fullerene (**18**) were investigated.[81] These conjugates were shown to be applicable in photovoltaics.[82—84] The charge separation rate constants for these systems are in the range of 10^9—10^{11} s^{-1}, which is several orders of magnitude higher than those for the complexes based on aluminum(III) porphyrinates described previously.[20,80] It should be noted that k_{CR} for TTF-containing systems depends on the chain length of the substituents. Thus, the longer the substituent, the slower the charge separation. The lifetimes of the $TTF^{\bullet+}$—$C_{60}^{\bullet-}$ charge-separated state for these systems, which were determined by time-resolved EPR spectroscopy, are 60—130 ns. These studies showed that AlPorph are promising and convenient components for the construction of fullerene-containing systems with secondary electron donors.

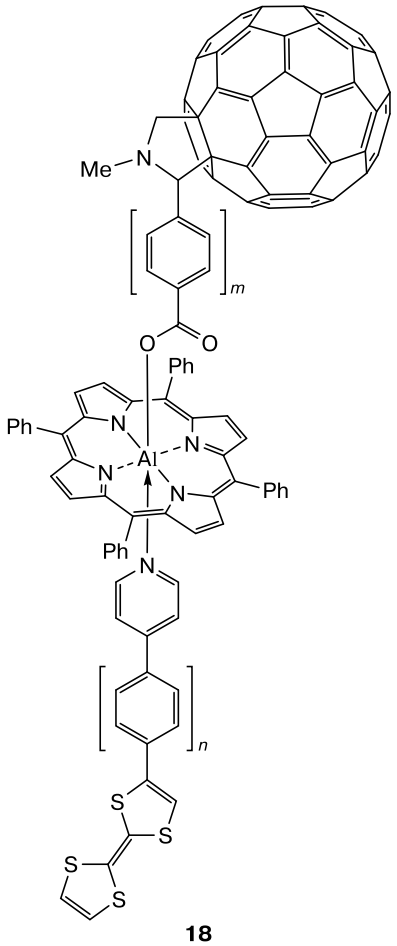

18

n, *m* = 1, 2, 3

A three-component multichromophoric system (**19**) containing aluminum(III) porphyrinate covalently linked to fullerene and ruthenium(II) porphyrinate as the secondary donor was constructed in the study.[21] The authors confirmed the occurrence of the stepwise photoinduced electron and positively charged particle transfer giving rise to a charge-separated state. Despite the fact that this system does not show outstanding characteristics (Table 2), it provides an insight into the effect of the secondary donor on the physicochemical properties of multichromophoric triads.

Table 2. Parameters of the charge transfer processes in three-component multichromophoric system **19** in different solvents

Solvent	ε	τ_1/ps	τ_2/ps
Dichloromethane	8.9	10	75
Tetrahydrofuran	7.6	20	80
Toluene	2.4	15	90

Note. ε is the dielectric constant, τ_1 is the primary charge separation time, τ_2 is the secondary charge separation/positive charge transfer time.

Macroheterocyclic complexes with tin(IV) as an oxophilic metal[85] are the same convenient building blocks for the preparation of fullerene-containing conjugates as aluminum porphyrinates/phthalocyaninates. Triad **20** is the first example of the tin(IV) porphyrinate complex (SnPorph) and fullerene linked by axial Sn—O bonds.[23] In this system, fullerenes are located on both sides of the macrocycle plane. This triad was characterized by diverse spectroscopic methods (UV-Vis, fluorescence, IR, and

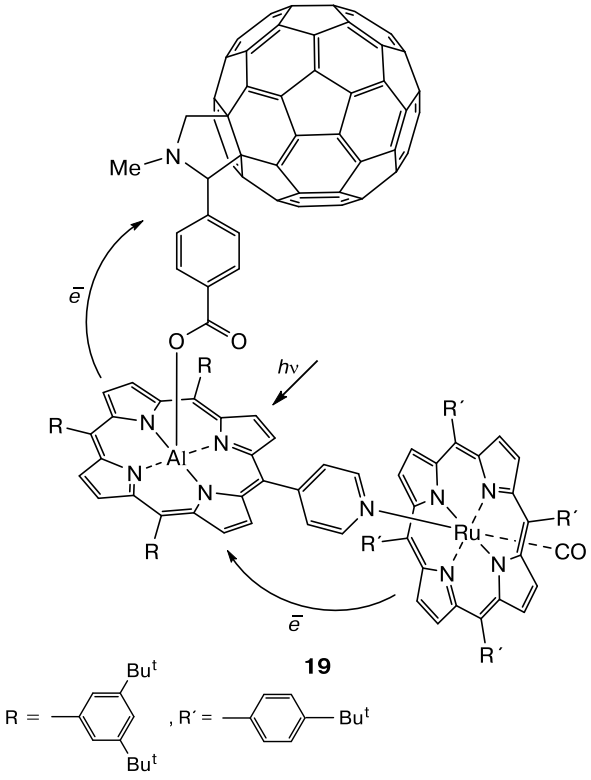

19

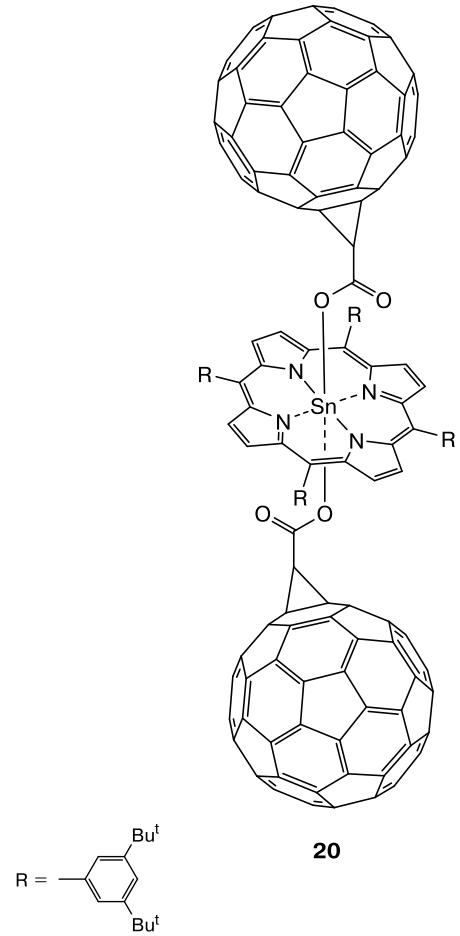

20

NMR spectroscopy and mass spectrometry) and elemental analysis. The ^{1}H NMR spectrum shows upfield shifts of signals of protons belonging to bridging groups between the porphyrin and fullerene components of the molecule. In the IR spectrum, the characteristic frequencies of the C=O bonds are shifted from 1700 cm^{-1} for free SnPorph to 1667 cm^{-1} in triad **20**, which is evidence of the presence of the carboxylate bond between metalloporphyrin and fullerene. The structure of this triad was established by X-ray diffraction, which confirmed the 1 : 2 stoichiometry.

An analysis of the fluorescence spectra of triad **20** and dibenzoate SnPorph as the reference compound shows that there is strong π—π interaction between the donor and acceptor units in the molecule. The fluorescence intensity of the triad is 140 times lower than that of free porphyrin. The time-resolved transient absorption spectra of the triad in toluene and benzonitrile show am extremely fast energy transfer with the lifetime of 2.7 and 3.0 ps, respectively.

In was noted[23] that triad **20** provides a new understanding of the design of artificial photosynthetic systems. In these structures, each fullerene unit is axially linked to tin(IV) porphyrinate through a covalent Sn—O bond. Porphyrin—fullerene conjugates were fabricated as nanowires by the addition of *trans*-dicarboxylate-substituted fullerene in a DMSO—chloroform system to a solution of tin(IV) porphyrinate in chloroform. The length of the nanowire varied from 50 to 300 nm, the time of the synthesis was 72 h, and the yield of the product was 58%. It is worth noting that this was the first study of nanowires by NMR spectroscopy. The ^{1}H NMR spectrum of the nanowire is characterized by a broadening of the signals of porphyrin protons and the absence of a signal at δ 7.48, which was assigned to the axial OH ligand in the spectrum of free SnPorph. The ^{119}Sn NMR spectrum shows a signal at δ –613.2 shifted upfield by 61 ppm with respect to the signal for tin(IV) in metalloporphyrin measured before the reaction with substituted fullerene. In the ^{13}C NMR spectrum, significant shifts of the signals of the fullerene cage confirm the formation of the nanowire. The morphology and sizes of the nanowire were determined from the images of this structure obtained by scanning tunneling and transmission electron microscopy. The successful synthesis of this compound allows the design and fabrication of nanomaterials based on macroheterocycles and fullerenes. Due to the strong electronic coupling between donors and acceptors and the favorable arrangement of the components, this conjugate can be considered as a promising system for the development of new π-electron nanomaterials for photovoltaic devices.

Silicon is also an oxophilic p-element and its macroheterocyclic complexes can serve as donor platforms for the construction of covalently linked conjugates with fullerenes.[86—91] Silicon phthalocyaninates (SiPc) have attracted attention due to their high solubility in organic media and the absence of aggregation.[87] All the synthesized systems are 1 : 2 triads. The synthesis of complex **21** with a chemical structure suitable for intramolecular photoinduced electron transfer (closely spaced fullerene and macrocycle), showing no aggregation in solution, was reported.[87] The fluorescence intensity of triad **21** was much lower than that of free silicon phthalocyaninate, which is indicative of efficient quenching of the singlet excited state of fullerene (the fluorescence quenching constant is $3.3 \cdot 10^9$ s^{-1}). The appearance of the charge-separated state was confirmed by time-resolved femtosecond transient laser flash photolysis measurements. The differential absorption spectra measured at different delay times in benzonitrile show bands at 880 and 1000 nm assigned to $SiPc^{\bullet+}$ and $C_{60}^{\bullet-}$ components, respectively, which is indicative of the formation of a charge-separated state. The rate constant of formation of $SiPc^{\bullet+}$ is $3.2 \cdot 10^9$ s^{-1}, being in good agreement with the fluorescence quenching rate constant. The lifetime of the charge-separated state is 5 ns. This value is rather large for structures based on metallophthalocyanines in polar solvents.

Systems based on silicon phthalocyaninate and fullerodendrimers containing 2, 4, or 8 fullerene substituents were synthesized[86] in order to increase the lifetime of the

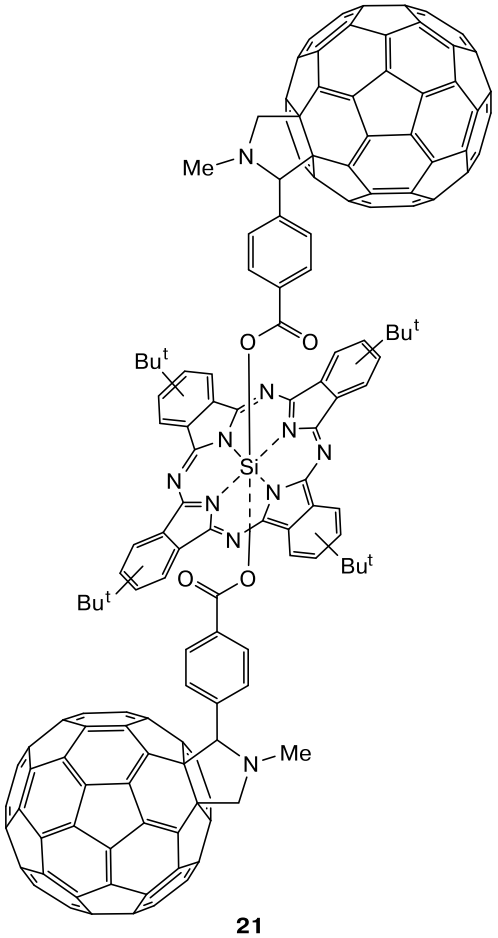

21

radical ion pair. The lifetime of the charge-separated state in polar (benzonitrile) and nonpolar (toluene) solvents rises with increasing generation of the axially coordinated fullerene-containing ligand. The largest value of τ_{RIP} (160 ns in nonpolar solvents and 200 ns in polar solvents) was observed for a third-generation system containing eight fullerene units, four units being on each side of the silicon phthalocyaninate.

The structures based on silicon macroheterocyclic complexes have attracted attention due to the competitive charge separation. The photophysical characteristics of multimodular donor-acceptor conjugates (**22** and **23**) were determined. In these triads, silicon phthalocyaninate acts as an electron donor and tetrachloroperylene diimide (PDI) and fullerene C_{60}, placed at the opposite ends of the silicon phthalocyaninate axial positions, serve as two electron donors.[91,92] In system **23**, the involvement of the fullerene entity in the electron transfer was seldom observed irrespective of which entity of the conjugate was excited and regardless of the solvent nature.[91] The competitive charge separation in conjugate **22** occurred with the participation of the acceptors PDI and C_{60} both in polar and nonpolar solvents upon PDI excitation.[92] Molecular systems **22** and **23** are of practical and fundamental interest, allowing the determination of the factors that influence the energy and electron transfer processes in such multimodular systems.

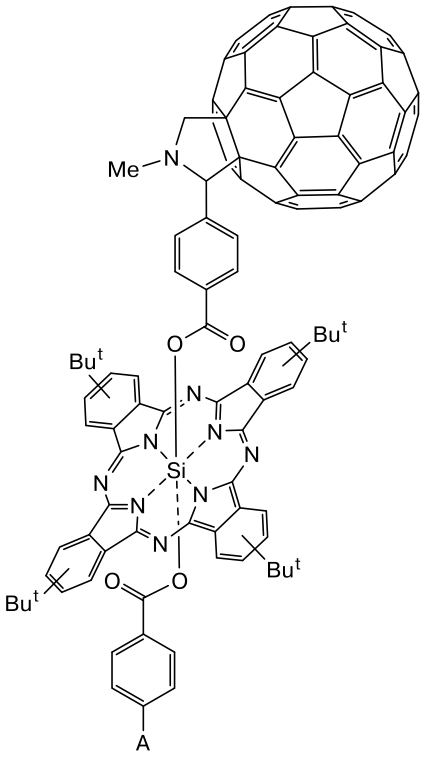

22, 23

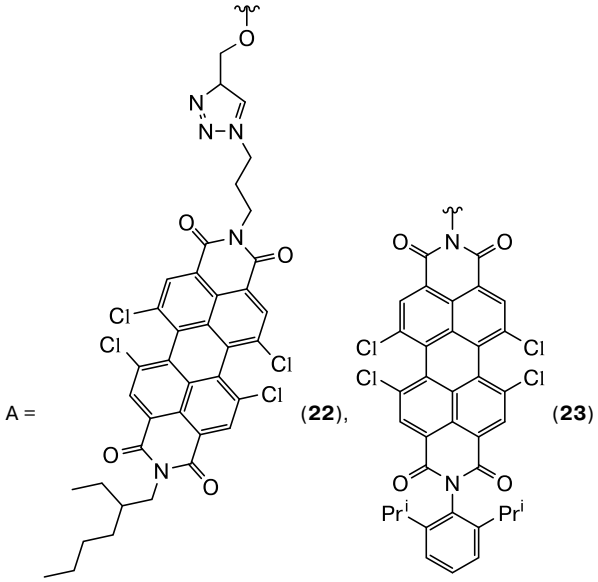

Covalent systems, in which d-metal porphyrinates/phthalocyaninates act as electron donors, were considered in numerous publications.[93–98] The prospects of the practical application of the above-described conjugates are related to the design of photoactive molecular materials for photovoltaics and optoelectronics, while conjugates based on iron(III) porphyrinates (FePorph) are of interest

as materials for biochemical, biomedical, and pharmaceutical applications.[94,99] Conjugate **24** based on FePorph was bound to apomyoglobin (the protein part of myoglobin) to form a conjugate-modified myoglobin.[94] Water-soluble fullerenes exhibit biological activity[100–102] against HIV,[103] herpes simplex virus, and cytomegalovirus.[104] Consequently, the introduction of a fullerene entity into water-soluble biomolecules is a possible strategy for the production of biomaterials with desired properties. Myoglobin modified by conjugate **24** was characterized by means of photoelectrochemical measurements. Thus, the cyclic voltammogram of a graphite electrode modified with compound **24** showed two pairs of reversible peaks, which can be assigned to the oxidation and reduction of the central iron cation (Fe^{2+}/Fe^{3+}) and the porphyrin ring. It is worthy of note that at electrodes modified by a film of the synthesized compound, an anodic current coupled with on-off UV light irradiation was observed at a potential below –0.2 V. This value is close to the Fe^{2+}/Fe^{3+} redox potential in the conjugate-modified myoglobin. The maximal photocurrent was 1.56 μA at –0.85 V. These studies open a way to constructing biomaterials based on conjugate-modified proteins.

The prospects of the use of the conjugate based on FePorph and fullerene for medical applications, in particular for the targeted delivery of a paramagnetic stable magnesium isotope to the doxorubicin-induced damaged heart muscle, were demonstrated in the study.[99] Biochemical and pharmacological assays of the synthesized conjugate in the rat myocardium affected by the doxorubicin-induced hypoxia is a part of the broader research aimed at developing pharmacological agents to prevent local tissue hypoxia. It was found that conjugate **25** is low-toxic and behaves as a "smart nanoparticle" capable to release magnesium ions $^{25}Mg^{2+}$ in response to pH. The drug delivery was accomplished by the multiple long-term administration of low drug doses, thereby providing a prophylactic or therapeutic effect in doxorubicin-induced hypoxia.

Nickel and copper macroheterocyclic complexes have also attracted attention as donor platforms for the preparation of covalently linked fullerene conjugates. In one of the pioneering studies aimed at preparing such conjugates, a system based on substituted nickel(II) phthalocyaninate (**26**) and fullerene C_{60} was synthesized by the Diels—Alder reaction.[95] After the long-term synthesis (4 days) and subsequent purification, the final product was obtained in a good yield (75%). The ^1H NMR spectrum of conjugate **27** showed some changes compared to the starting phthalocyanine (NiPc). Thus, signals of protons of exocyclic bonds were absent and a new signal of methylene protons appeared as a multiplet along with signals of heptyl groups. Figure 1 presents the UV-Vis spectrum of the starting NiPc and conjugate **27**. It can be seen that the formation of the conjugate results in the splitting of the *Q* band of Pc with maxima at 679 and 699 nm.

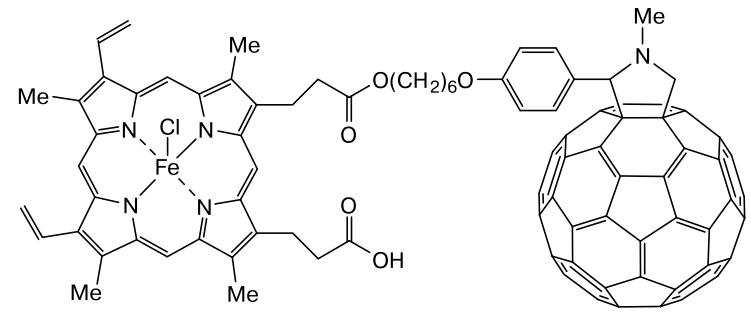

24

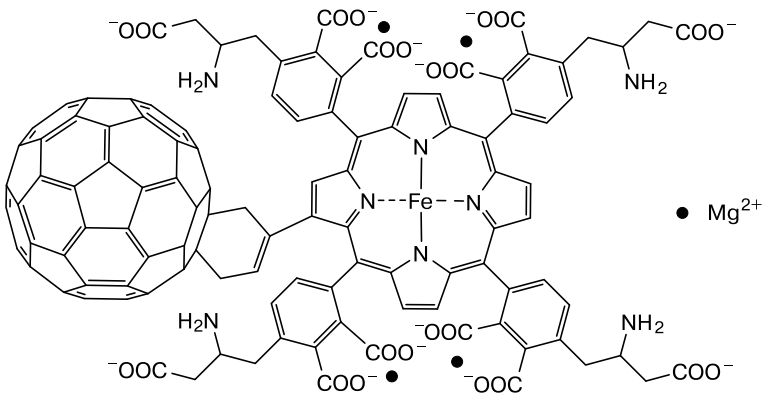

25

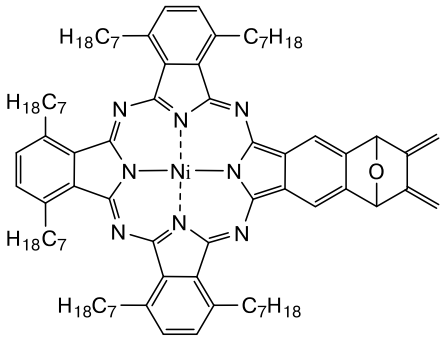

26

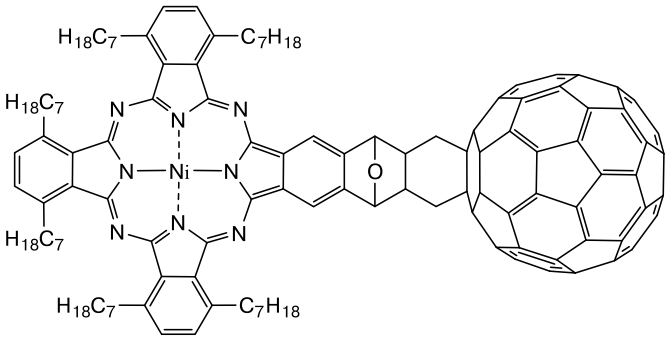

27

The electrochemical behavior of conjugate **27** was characterized in the study.[95] The cyclic voltammogram displays five reversible reduction peaks at −0.41, −0.81, −0.90, −1.26, and −1.53 V. The reduction potentials of nickel(II) phthalocyaninate differ only slightly from those mentioned above, and the reduction of the fullerene entity shows a pronounced optical response in the UV-Vis spectrum. The authors ruled out the charge transfer in conjugate **27** under ambient environmental conditions.

The synthesis of fullerene-containing conjugates based on nickel(II) and copper(II) complexes with *meso*-aryl-substituted porphyrins containing long-chain alkyl groups was reported in the study.[68] Conjugates **28** were prepared from the corresponding formyl derivatives of metalloporphyrins and fullerene C_{60} by the Prato reaction (Scheme 3). These conjugates have attracted attention in relation to the design of artificial photosynthetic systems and the possibility to expand the class of such nanostructured materials as thermotropic liquid crystals.

Covalently linked assemblies based on copper(II), nickel(II), and cobalt(II) phthalocyaninates and fullerene (**29—33**) were synthesized.[93,96—98] These systems have liquid-crystalline properties and are able to undergo photoinduced charge transfer.

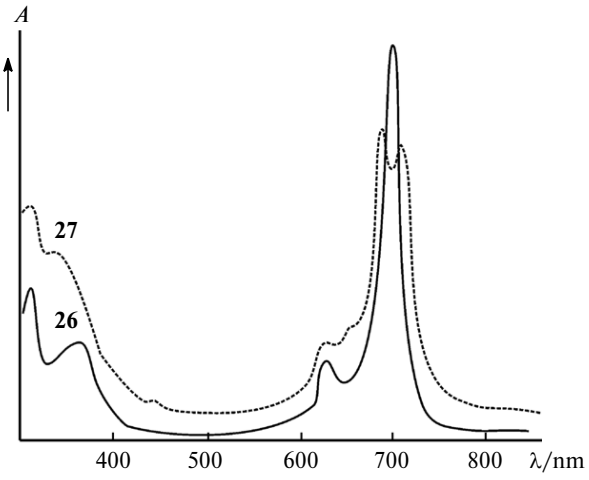

Fig. 1. Electronic absorption spectra of nickel phthalocyaninate **26** and its conjugate with fullerene **27** in toluene.[95]

Liquid-crystalline compounds containing electron donor and acceptor units are used as photoactive films in organic solar cells.[108] The capability to undergo homeotropic orientation may be particularly beneficial for photoelectrochemical conversions of solar energy into electricity due to strong π—π stacking.[109] Conjugate **29** shows a perfect homeotropic alignment; however, the yield of this compound was low (about 20%). Hence, conjugates **30** were synthesized by the Prato reaction,[53] instead of the Bingel reaction,[110] resulting in high yields of the target products (up to 81—96%). Conjugates **30** also exhibit an ideal homeotropic alignment in the tetragonal columnar phase at high temperatures.[111] The removal of the methoxy group in conjugates **31** synthesized by the Prato reaction make the compounds capable of forming homeotropic orientation at lower temperatures.[106] It should be noted that complexes based on free Pc and copper phthalocyaninate show only one tetragonal columnar mesophase.

Compounds **32** were synthesized in order to elucidate the effect of the spacer chain length (n = 6, 8, 10, 12) on the mesomorphism.[105] The conjugates based on copper(II) phthalocyaninate (CuPc) with short spacers (n = 6, 8) show a hexagonal columnar mesophase, whereas the conjugates with long spacers (n = 10, 12) based on copper(II), nickel(II), and cobalt(II) phthalocyaninates exhibit a tetragonal columnar mesophase. As part of efforts to develop approaches to the design of photoactive components based on liquid-crystalline conjugates for solar cells, new dyads **33** were prepared. These dyads show a homeotropic alignment in the hexagonal mesophase between two glass plates.[107] Since none of the starting metallophthalocyanines showed this alignment, the authors suggested that this is due to a strong affinity between fullerene and the glass surface as a result of the formation of a helical supramolecular system. This method is efficient for the molecular design of homeotropic alignment-showing discotic liquid crystals.

Ishikawa *et al.*[93] synthesized new discotic columnar liquid crystals based on phenoxy-substituted CuPc containing the same linear alkoxy group ($C_{16}H_{33}$) at different

Scheme 3

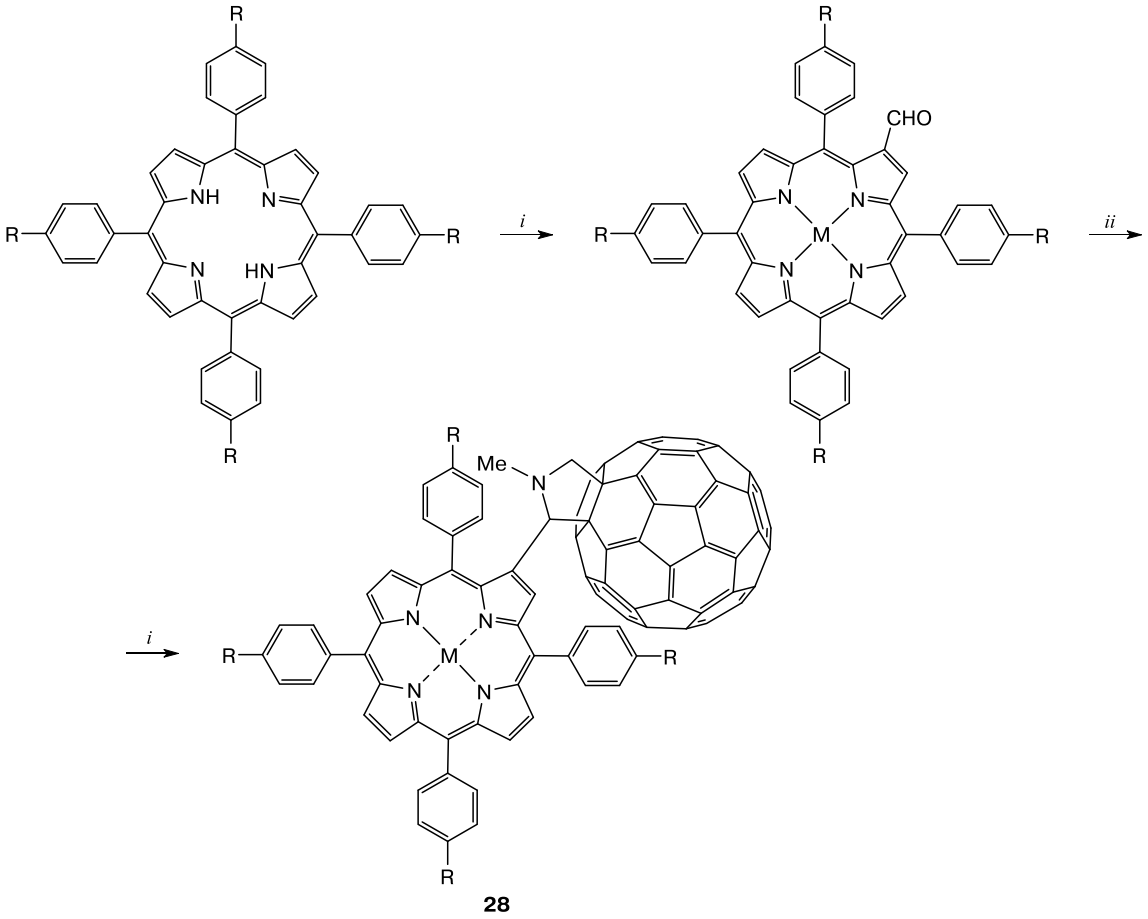

R = $O(CH_2)_{13}Me$; M = Ni, Cu

i. 1) $NiCl_2/Cu(OAc)_2$, MeOH, $CHCl_3$; 2) DMF and $POCl_3$, $CHCl_3$; *ii*. C_{60}, *N*-methylglycine, toluene, Ar.

positions of the phenoxy group (only in the *meta* or *para* position or simultaneously in both positions). The investigation of the mesomorphism of these compounds by differential scanning calorimetry, X-ray diffraction, and polarized optical microscopy demonstrated the formation of columnar mesophases. Generally, the homeotropic alignment was observed for derivatives containing substituents both at the *meta* and *para* positions. The authors noted that the *meta*-substituted derivatives containing long alkoxy chains (conjugate **34**) are suitable for the formation of a helical supramolecular structure. The elucidation of the relationship between the molecular structure of the conjugates and their liquid-crystalline properties is an important step in the development of molecular materials with required properties.

In a simple covalently linked dyad, the charge separation occurs from the excited singlet state* of the sensitizer. Obondi *et al.*[97] developed an alternative approach to improve the photophysical characteristics using the high-energy triplet state. For this purpose, the authors prepared porphyrin—fullerene dyads containing palladium(II) and platinum(II) porphyrinates (PdPorph and PtPorph) as electron donors. The synthesis involved several steps: the formation of Porph, its formylation, the complexation using palladium acetate $PdAc_2$ or platinum chloride $PtCl_2$, and the synthesis of fullerene conjugates by the Prato reaction.

The energies of the excited triplet states of heavy metal porphyrinates are rather high (1.89 and 1.84 eV for Pd^{II} and Pt^{II} porphyrinates, respectively). The use of these compounds as photosensitizers facilitates the fast intersystem crossing process. However, the photoinduced electron transfer from short-lived singlet or long-lived triplet excited states of metalloporphyrins to fullerene did not occur, as evidenced by the absence of characteristic absorption bands in the differential absorption spectra at different delay times. Nanosecond absorption spectroscopy measurements demonstrated the triplet-triplet energy

* Hereinafer, the excited singlet state is indicated by the superscript 1.

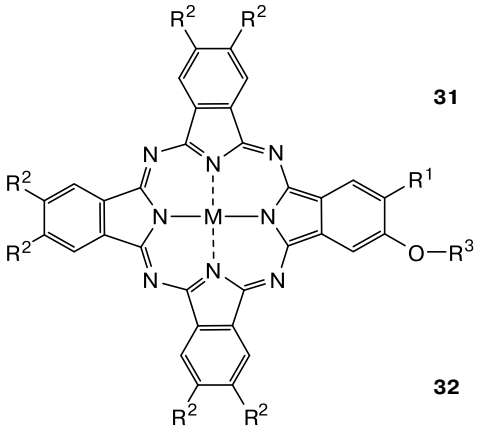

29—34

Compound	M	R^1	R^2	R^3
29	Cu	OMe	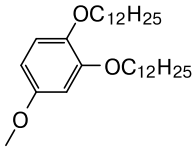	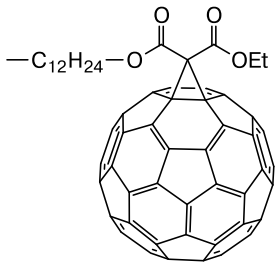
30	Co, Ni, Cu	OMe	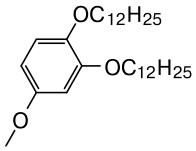	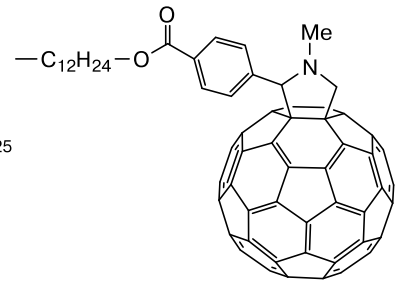
31	Co, Ni, Cu	H	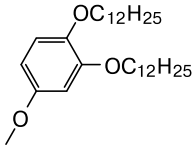	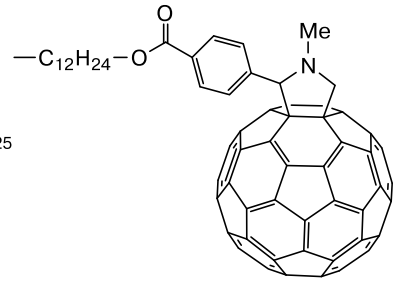
32	Co, Ni	H	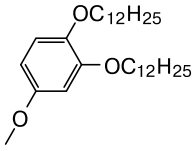	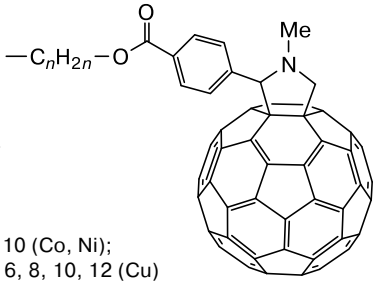 *n* = 10 (Co, Ni); 6, 8, 10, 12 (Cu)
33	Cu	H	$-SC_nH_{2n+1}$ (*n* = 14, 16, 18)	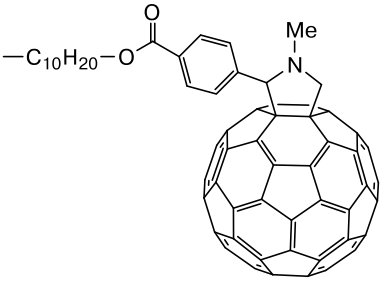
34	Cu	H	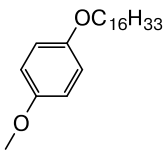	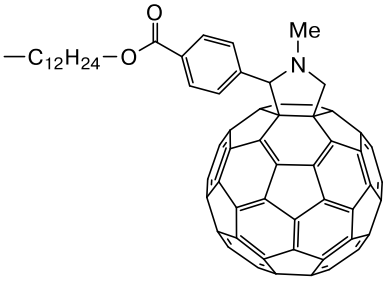

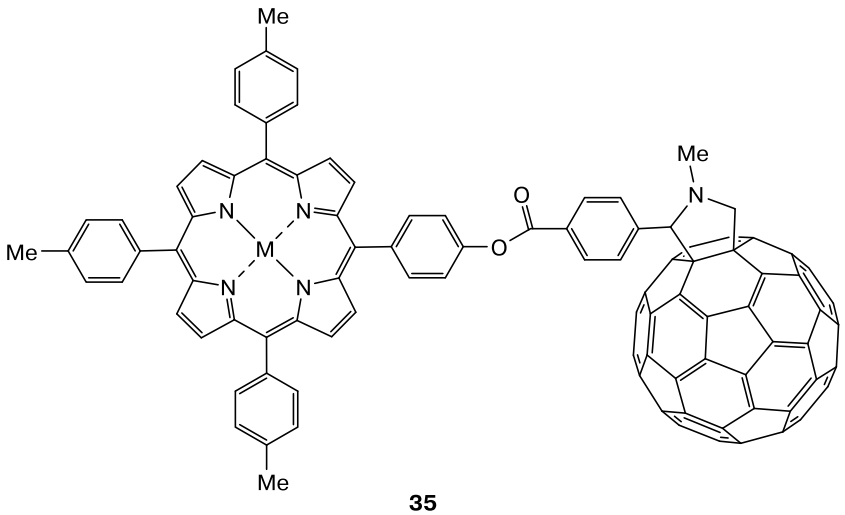

35

M = Pd, Pt

transfer from the triplet excited state of metalloporphyrin to fullerene in dyads **35**. This gave impetus to further research on the synthesis[98] of conjugates based on porphyrins of heavy metals, in particular Pd^{II} (conjugates **36** and **37**).

To bring the donor and acceptor into close proximity, fullerene in dyad **36** is linked to PdPorph *via* the β position. This approach enables an increase in the rate of electron transfer from the excited palladium porphyrinate to fullerene. Triphenylamine (TPA) substituents at the periphery of the porphyrinate macrocycle in conjugate **37** were introduced in order to stabilize $PdPorph^{\bullet+}$. This, in turn, influences the electron transfer through the triplet-triplet excited state. The above-considered approaches to the design of systems, in which the triplet electron transfer leads to the long-lived charge-separated state, were found to be promising. This system is of interest as a potential photocatalyst. Consequently, investigations of the mechanisms of charge separation in the $[Pd(TPA)_3Porph]^{\bullet+}$—$C_{60}^{\bullet-}$ system are ongoing.[112]

Covalently linked Porph/Pc—C_{60} conjugates are promising components of photoactive, medical, and pharmaceutical materials. Meanwhile, there are other approaches to the synthesis of systems simultaneously containing a donor (a macroheterocyclic complex) and an acceptor (fullerene), namely the formation of supramolecular systems. Before proceeding to the discussion of the diversity of supramolecular systems and the ways of their formation, let us mention the publication,[113] in which the donor-acceptor binding of two dyads (**38** and **39**) was shown to have advantages over covalent binding.

It was found that the azulenocyanine-centered excited state in covalently linked dyad **39** does not enhance elec-

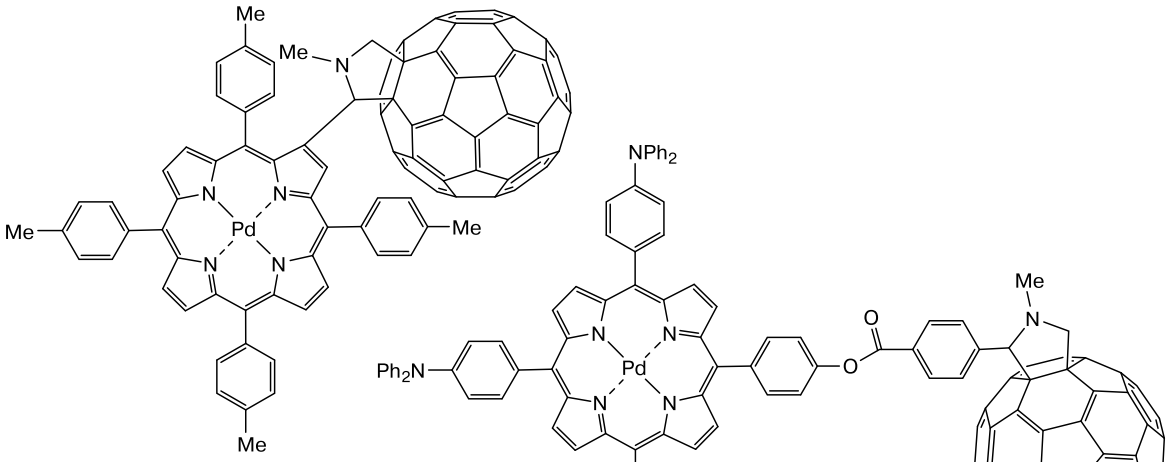

36

37

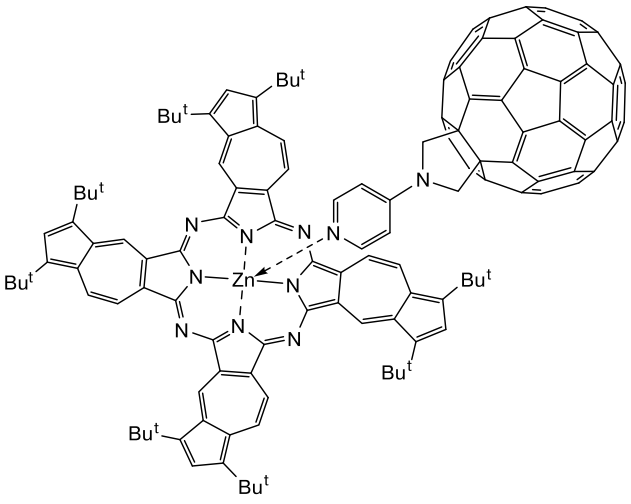

38

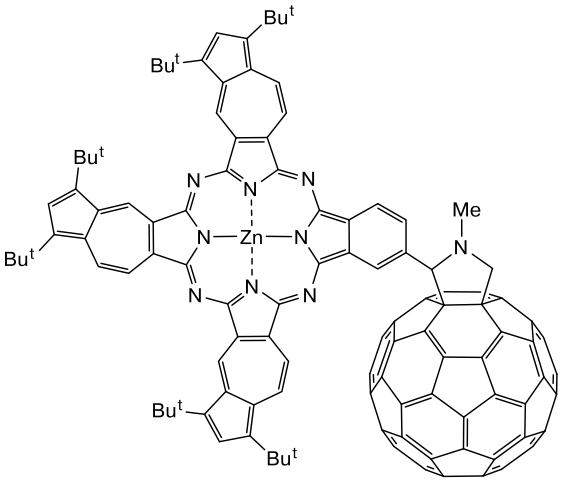

39

tron transfer upon photoexcitation. The electron transfer was not observed because the excited state is spread over the azulene moiety of the macrocycle, while the electron-accepting fullerene is linked to the isoindole entity of the molecule. On the contrary, the photoinduced electron transfer occurs in donor-acceptor system **38**. The results of these study demonstrate the importance of the appropriate choice of the strategy for the synthesis of systems capable of exhibiting photoinduced charge separation. The efficient approach to the synthesis of supramolecular systems through metal—nitrogen coordination bonding is considered in detail below.

2. Supramolecular systems based on s-, p-, and d-metal macroheterocyclic complexes and fullerenes

First studies on the synthesis of supramolecular systems based on macroheterocyclic complexes and fullerenes dated back to the end of the 20th century. Various supramolecular systems based on zinc porphyrin and phthalocyanine complexes with fullerenes were studied in most detail. These systems are stabilized by non-covalent bonds, such as hydrogen bonding,[114,115] crown ether—ammonium ion binding,[116,117] electrostatic interactions,[118,119] anionic interactions,[121] and axial metal—ligand coordination.[122—125] In recent years, porphyrin and phthalocyanine complexes with other s-, p-, and d-metals have captured the attention of researchers. The use of such complexes as donor platforms may expand the possibilities of designing supramolecular systems with valuable properties.[126—128]

In the beginning of the 21th century, molecular complexes of fullerenes (C_{60}/C_{70}) with metalloporphyrins (cobalt(II), nickel(II), copper(II), and iron(III) octaethylporphyrinates (OEP)) were prepared relying on relatively weak (compared to the classical covalent chemical bonds) van der Waals interactions.[126] Their structures were established by X-ray diffraction. It was found that the molecular complexes $C_{60}\cdot 2CoOEP\cdot CHCl_3$ and $C_{60}O\cdot 2CoOEP\cdot \cdot CHCl_3$ containing one C_{60} molecule surrounded by two metalloporphyrin molecules were formed by the interaction of CoOEP with C_{60}, whereas the 1 : 1 complexes ($C_{70}\cdot CoOEP\cdot C_6H_6\cdot CHCl_3$, $C_{70}\cdot NiOEP\cdot C_6H_6\cdot CHCl_3$, $C_{70}\cdot CuOEP\cdot C_6H_6\cdot CHCl_3$, and $C_{60}O\cdot ClFeOEP\cdot CHCl_3$) were produced in other cases.[126]

Molecular complexes of composition 1 : 1 were prepared by evaporation of solutions containing fullerene (C_{60}/C_{70}) and the appropriate Mn^{II}, Co^{II}, Cu^{II}, Ni^{III} tetraphenylporphyrinate (M/TPP).[128] It was found that the ability to form porphyrin—fullerene dyads depends on the solvent nature. Thus, the complex of fullerene with Mn(TPP) was prepared only in CS_2, the complexes with Cu(TPP) and Co(TPP) were obtained in benzene and toluene, whereas attempts to isolate the complex with nickel tetraphenylporphyrinate were unsuccessful. All M(TPP)—C_{60} complexes are well-formed crystals, some of which slowly decompose in air or even under an argon atmosphere due to the loss of the solvent, *i.e.*, they are unstable. These systems were studied by EPR, IR, UV-Vis, and X-ray photoelectron spectroscopy, which demonstrated that no significant charge transfer from porphyrinate to fullerene molecules occurred.[128]

Fullerene-containing triads based on Jaw-like Pd, Zn, Cu, Co, Fe, Mn bis(metalloporphyrinates) (M_2JawsPorph) were synthesized.[18] These triads contain two palladium-linked metalloporphyrins (**40**). The host—guest complexation with fullerene C_{60} was studied in toluene. The Soret bands of metalloporphyrins were bathochromically shifted (up to 7 nm). The binding constants for C_{60} and M_2JawsPorph were determined by variable-temperature ^{13}C NMR spectroscopy in toluene-d_8 (Table 3). The affinity of M_2JawsPorph for C_{60} increases in the series $Fe^{II} < Pd^{II} < Zn^{II} < Mn^{II} < Co^{II} < Cu^{II} < 2H$. Quite unexpectedly, porphyrin H_2JawsPorph was found to be

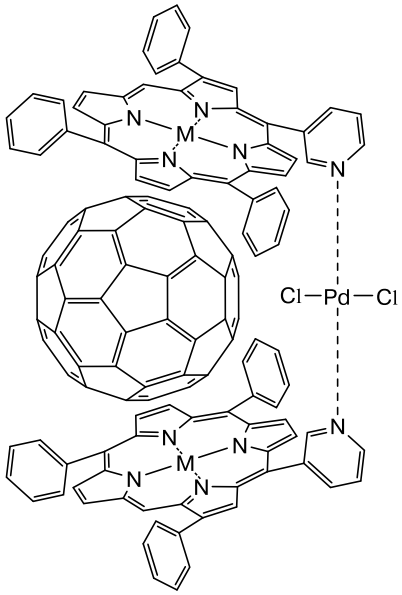

40

stronger linked to fullerene compared to metalloporphyrins. The authors attributed this fact to electrostatic attraction between C_{60} and the electropositive site of porphyrin, assuming that the van der Waals attractive forces are not constant in the series of metalloporphyrins. A different degree of porphyrin distortion leads to a change in the contact surface area with fullerene, thereby facilitating the change in the van der Waals term and the binding energy. The principles of supramolecular assembly deduced from these studies offer new possibilities for assembling discrete supramolecular complexes and highlight the potential application to control the photophysical properties and the charge transfer in single-molecule magnets and molecular conductors and to construct of new porous metal-organic frameworks.

The development of efficient methods for the synthesis of supramolecular systems made it possible to observe the coordination of fullerene radical anions to cobalt(II) tetraphenylporphyrinates (CoTPP). In 2003, the multicomponent ionic complex $CoTPP \cdot 2C_{60}(CN)_2 \cdot 2Cr(C_6H_6)_2 \cdot 3C_6H_4Cl_2$, where $Cr(C_6H_6)_2$ is bis(benzene)chromium and $C_6H_4Cl_2$ is 1,2-dichlorobenzene, was synthesized. The crystal of this complex suitable for X-ray diffraction was obtained under an inert gas atmosphere by the diffusion of hexane into a solution of fullerene, CoTPP, and $Cr(C_6H_6)_2$ in 1,2-dichlorobenzene. According to the crystallographic data, one $C_{60}(CN)_2$ molecule is covalently linked to CoTPP (the Co···C_f distance is 2.28 Å), whereas the second $C_{60}(CN)_2$ molecule in involved in a van der Waals interaction with CoTPP (the Co···C_f distances are 2.79 and 2.93 Å).[129]

Table 3. Stability constants of supramolecular triads (**40**) based on bis(metalloporphyrins)[18]

Metal (M)	β/L mol^{-1}	Metal (M)	β/L mol^{-1}
Fe^{2+}	490±15	Co^{2+}	2975±120
Pd^{2+}	815±120	Cu^{2+}	4860±250
Zn^{2+}	1945±750	2H	5200±120
Mn^{2+}	2760±120		

In the multicomponent ionic complex $(CoTPP(C_{60}))_2 \cdot 1.7Cr(C_6H_6)_2 \cdot 3.3C_6H_4Cl_2$,[130] the Co···$C_f$ bond lengths are 2.29—2.32 Å. The smaller Co···C_f bond lengths in the ionic complexes compared to the molecular complexes of fullerenes with cobalt(II) porphyrinates (2.55—3.00 Å)[126,131] indicate that the fullerene radical anions are stronger ligands compared to the neutral C_{60} molecules. The σ-binding of fullerene is attributed to the presence of an additional electron on its π* level, which interacts with the dz^2 orbital of cobalt(II) porphyrinate. According to the UV-Vis and IR spectra, fullerene in these complexes is in the monoanionic state.[130]

Various coordination assemblies of molecular and ionic complexes based on metalloporphyrins or metallophthalocyanines with neutral and negatively charged fullerenes are summarized in the review.[132]

Supramolecular systems can also be prepared through self-assembly processes based on s-, p-, and d-metal porphyrinates or phthalocyaninates and fullerenes involving axial metal—ligand coordination. In the first review[3] devoted to photoactive donor-acceptor systems with this binding mode, the synthesis of supramolecular dyads and triads based on ZnPorph or ZnPc as the donor and fullerenes as the acceptor was described in detail. These supramolecular assemblies are still attracting attention. The functionalization of the donor and acceptor entities of the system leads to an increase in the lifetime of the charge-separated state and retardation of the charge recombination, which is very important for their further practical application.[1,9]

The photoinduced electron transfer through the axial metal—ligand coordination within the supramolecular system was studied using fullerenes (C_{60}/C_{70}) functionalized with pyridyl (Py) or phenylimidazole (Im) groups (**I—III**). These groups enhance the solubilization of fullerenes in organic media and, consequently, facilitate the

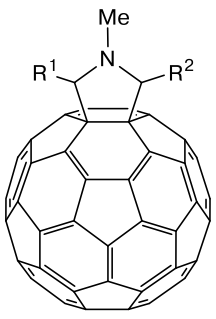

I

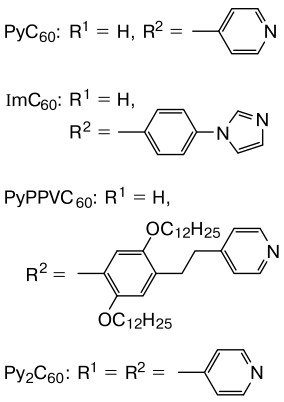

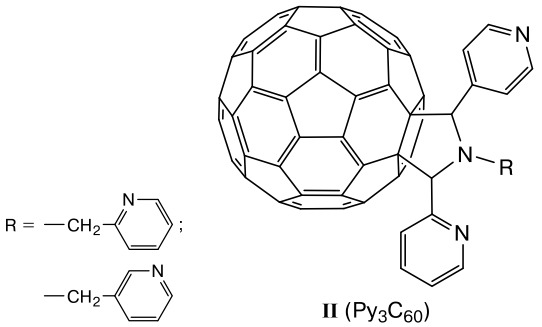

II (Py_3C_{60})

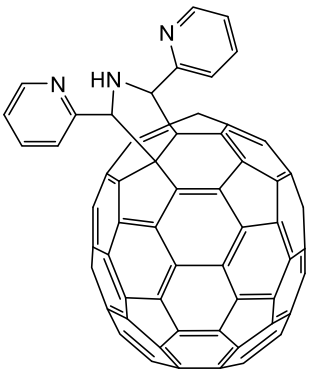

III (Py_2C_{70})

study of the reactions with their participation. Besides, fullerene derivatives exhibit excellent electron-withdrawing properties because the charge delocalization over their spherical structure stabilizes the unpaired electron, resulting in low reorganization energies.[133]

An analysis of supramolecular systems demonstrated that their photochemical properties are controlled not only by the binding mode of the components of the system but also by the solvent nature, in which the self-assembly occurs, the nature of functional substituents of macroheterocyclic compounds and fullerenes, and the steric factors. The metal ion in the Porph/Pc plane also plays an important role, thereby making it possible to study the effect of the structure on the reactivity of supramolecular systems and their ability to exhibit photoinduced charge separation. Magnesium *meso*-tetraphenylporphyrinate (MgTPP) was used as the donor for the construction of the porphyrin—fullerene dyad.[15] This compound has a number of advantages over zinc porphyrinates. Thus, it has a higher fluorescence quantum yield and a longer excited-state lifetime[15] and can bind up to two axial ligands,[134] as opposed to zinc porphyrinates coordinating only one axial ligand. The composition of the donor-acceptor complex MgTPP with ImC_{60} was determined by spectrophotometric titration. It was shown that the synthesis afforded five-coordinate complex **41** with a stability constant of $9.2 \cdot 10^3$ L mol^{-1}.[15] Attempts to synthesize the six-coordinate complex $2ImC_{60} \cdot$ MgTPP and characterize it by spectroscopic methods failed, because higher concentrations of ImC_{60} are required for its formation, which interferes with the observation of the spectral features of MgTPP.

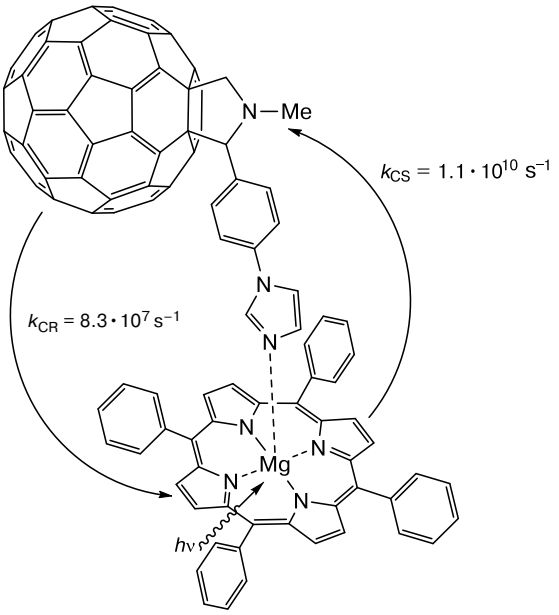

41

The molecular geometry and electronic structure of complex **41** were determined by quantum chemical calculations in terms of the density functional theory (DFT) using the three-parameter functional B3LYP and the 21G* basis set (B3LYP/3-21G*). In the optimized structure of the resulting dyad, the Mg←$N_{ImC_{60}}$ distance is 2.06 Å. The frontier molecular orbitals (HOMO and LUMO) are spread over the porphyrin and fullerene entities, respectively, which is indicative of the photoinduced electron transfer in the obtained system. The ratio of the charge separation to charge recombination rates in dyad **41**, which was evaluated by time-resolved emission and transient adsorption spectroscopy, respectively, is much higher compared to that for the $ImC_{60} \cdot$ ZnTPP dyad.[11] The decay constant $K_{SV} = 2.8 \cdot 10^4$ L mol^{-1} was determined by the fluorescence titration of MgTPP with ImC_{60} in 1,2-dichlorobenzene under an argon atmosphere and the data processing by the Stern—Volmer method. This constant is indicative of the efficient decay process with the rate constant $k_q = 5.6 \cdot 10^{12}$ s^{-1} and the lifetime of 5 ns for ^{1}MgTPP* and also confirms the occurrence of electron transfer in the dyad.

Among p-metal macroheterocyclic complexes, aluminum porphyrinates (AlPorph) and indium porphyrinates (InPorph) form donor-acceptor systems with fullerenes. Aluminum porphyrinates are of interest due to their ability to form five-coordinate complexes through the covalent binding of the metal center to carboxylic acids[135] or alcohols[136] and also six-coordinate complexes through the axial coordination of *N*-bases.[80] In the aluminum(III) porphyrinate molecule, the covalently linked ligand and

the ligand linked by the donor-acceptor interaction are located on opposite sides of the porphyrin plane. The geometry of this molecule provides an excellent opportunity to study the effect of the electronic coupling energy and reorganization energy on the energy and electron transfer in the perpendicular (axial) direction with respect to the porphyrin plane and also to solve a general problem often encountered in such porphyrin structures, namely, to prevent aggregation.[137] Triads **42**—**45** based on AlPorph were synthesized and characterized.[137] In these triads, 4,4-difluoro-4-bora-3a,4a-diaza-*s*-indacene (boron dipyrromethenate, BODIPY, BDP), bearing a hydroxy or carboxylate group and covalently linked to the aluminum center, served as an electron donor, and pyrrolidinyl-substituted fullerenes (PyC_{60} and $PyPPVC_{60}$, PyPPV is pyridine poly(*p*-phenylene vinylene)), linked to the metal center by a donor-acceptor interaction, served as electron acceptors. The stability constants of the supramolecular systems were determined by spectrophotometric titration. Their values for the triads with PyC_{60} (**42**, **44**) were found to be somewhat higher compared to the PyPPV—C_{60} triads (**43**, **45**).

Thermodynamic feasibility of the energy transfer from ^{1}BDP* to Al(TPP) and the subsequent electron transfer from ^{1}Al(TPPorph)* to generate the BDP-Al(TPP)$^{\bullet+}$—$C_{60}^{\bullet-}$ radical cation pair was derived from free-energy calculations of the charge separation ($-\Delta G_{CS}$) and charger recombination ($-\Delta G_{CR}$) using analysis of cyclic voltammograms and DFT quantum chemical calculations (B3LYP/6-31G*). The study by time-resolved transient absorption spectroscopy demonstrated that the BDP-Al(TPP)$^{\bullet+}$—$C_{60}^{\bullet-}$ charge-separated state persisted for a few nanoseconds prior to returning to the ground state.

Four supramolecular triads **46**—**49** were synthesized by the assembly of the appropriate aluminum(III) (3,4,5-trifluorophenyl)porphyrinate (Al(TPF_3Porph)) with imid-

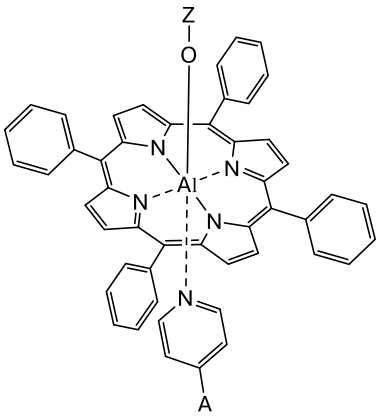

42—45

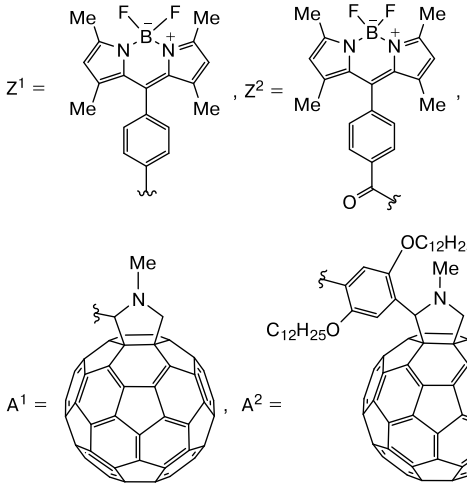

A = A^1, Z = Z^1 (**42**); A = A^2, Z = Z^1 (**43**); A = A^1, Z = Z^2 (**44**); A = A^2, Z = Z^2 (**42**)

Triad	A	Z	β/L mol^{-1}	$-\Delta G_{CR}$*/eV	$-\Delta G_{CS}$*/эВ
42	A^1	Z^1	$7.57 \cdot 10^3$	1.57	0.57
43	A^2	Z^1	$5.04 \cdot 10^3$	1.59	0.55
44	A^1	Z^2	$5.20 \cdot 10^3$	1.55	0.60
45	A^2	Z^2	$2.27 \cdot 10^3$	1.55	0.59

* The data from Ref. 137.

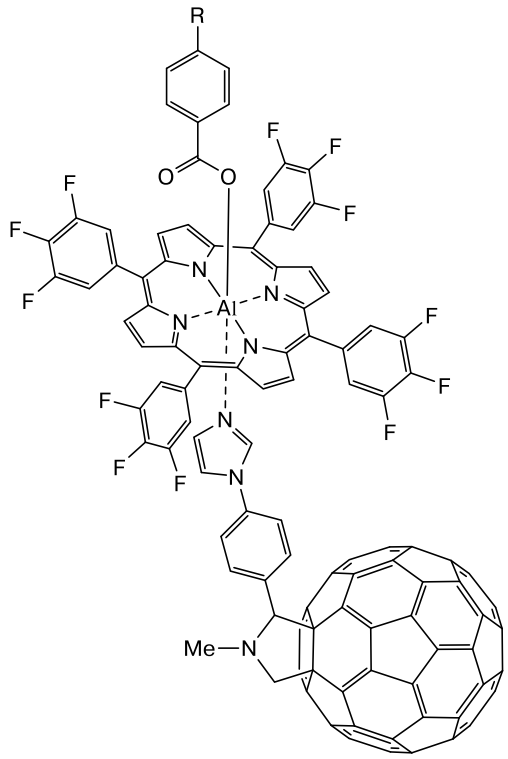

46—49

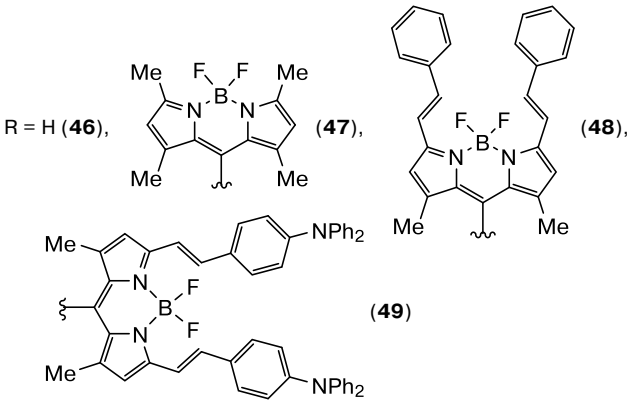

Table 4. Stability constants (β) and optical characteristics (λ = 545 nm) of spatially separated supramolecular triads **46—49**

Triad	β/L mol^{-1}	k_{CS}/s^{-1}	k_{EnT}*/s^{-1}
46	$1.38 \cdot 10^5$	$2.77 \cdot 10^9$	—
47	$1.03 \cdot 10^5$	$2.43 \cdot 10^9$	—
48	$5.99 \cdot 10^4$	$3.35 \cdot 10^9$	10^{10}
49	$8.81 \cdot 10^4$	$1.40 \cdot 10^{10}$	—

* k_{EnT} is the energy transfer rate constant.

azole-functionalized fullerene.[138] In these triads, the components are spatially well separated without any electronic interactions. Photoinduced processes in the triads were studied by steady-state fluorescence and femtosecond transient absorption spectroscopy. Diverse redox and optical properties of the entities in triads **46—49** allowed the investigation of the influence of the excitation wavelength on the photochemical process in the triads (Table 4). Thus, the excitation of the Al(TPF$_3$Porph) entity in triad **47** causes the electron transfer from ^{1}Al(TPF$_3$Porph)* to ImC$_{60}$ to form the BDP—Al(TPF$_3$Porph)$^{\bullet+}$ ← ImC$_{60}^{\bullet-}$ radical ion pair, whereas the excitation of the BDP entity induces rapid energy transfer from ^{1}BDP* to ^{1}Al(TPF$_3$Porph)*.

In triad **48**, the excitation of Al(TPF$_3$Porph) leads to the charge separation and subsequent consecutive electron transfers to form Ph$_2$-BDP—^{1}Al(TPF$_3$Porph)* ← ImC$_{60}$ → Ph$_2$-BDP—Al(TPF$_3$Porph)$^{\bullet+}$ ← ImC$_{60}^{\bullet-}$ → (Ph$_2$-BDP)$^{\bullet+}$—Al(TPF$_3$Porph)$_3$ ← ImC$_{60}^{\bullet-}$ radical pairs. However, the rate of the competitive energy transfer from ^{1}Ph$_2$-BDP* to ^{1}Al(TPF$_3$Porph)* is an order of magnitude higher that the charge separation rate. Hence, the excited state ^{1}Al(TPF$_3$Porph)* is strongly quenched. In triad **49**, the excitation of both the Al(TPF$_3$Porph) and TPA$_2$-BDP entities (TPA is triphenylamine) causes only the electron transfer giving rise to the charge-separated state (TPA$_2$-BDP)$^{\bullet+}$—Al(TPF$_3$Porph) ← ImC$_{60}^{\bullet-}$. Therefore, styryl-containing BDP derivatives improve the optical sensitivity of the supramolecular system as a whole, but their extended structure (additional functionalization with BDP) showed a modest influence on the stabilization of the final radical pair (BDP derivative)$^{\bullet+}$—Al(TPF$_3$Porph) ← ← (ImC$_{60}$)$^{\bullet-}$.

A supramolecular system TPE-Al(TPPorph) • ImC$_{60}$ utilizing tetraphenylethylene (TPE) as the secondary electron donor was characterized.[19] It was shown that the initial charge separation between TPE and Al(TPPorph) occurs with the formation of the high-energy state TPE$^{\bullet+}$—Al(TPPorph)$^{\bullet-}$ ← ImC$_{60}$ (2.14 eV), which undergoes the charge shift to ImC$_{60}$ to form the second high-energy state (1.78 eV) TPE$^{\bullet+}$—AlTPPorph ← ImC$_{60}^{\bullet-}$ with a lifetime of about 25 ns. Therefore, the triads based on aluminum(III) porphyrinates can be used as potential electron-transfer catalysts for high-energy photochemical reactions, particularly in the artificial photosynthesis as a path to convert solar energy into chemical energy.

Indium(III) porphyrinates (InPorph) provide another example of p-metal macroheterocyclic complexes capable of forming donor-acceptor systems with fullerenes.[139] These compounds are potential photosensitizers for photodynamic therapy and other photosensitive devices, such as organic light-emitting diodes and thin-film transistors. Indium porphyrinate displays the desired photophysical properties, such as a long lifetime of the excited triplet state, a short fluorescence lifetime, a low fluorescence quantum yield, and a high quantum yield of the singlet oxygen generation.[140] The study of (Cl)InTPPorph and axially substituted (X)InTTPorph (TTPorph is tetra-*p*-tolylporphyrin) with different axial ligands demonstrated that the axial ligands have a positive effect on the nonlinear optical properties of metalloporphyrins.[141] The cluster complexes of InPorph with Os$_3$(μ-H)$_2$(CO)$_{10}$ region were synthesized and characterized.[142] These compounds show promising synthetic characteristics for the sensor protection in the visible region.

Dyads **50** and **51** were constructed by the assembly of individual components of the system in CHCl$_3$ and toluene, respectively.[25,26,143] The stability constants of supramolecular dyads **50** and **51**, evaluated by spectrophotometric titration, are $2.3 \cdot 10^3$ and $6.9 \cdot 10^4$ L mol^{-1}, respectively. The equilibrium constants of the formation of porphyrin—fullerene dyads based on unsubstituted (Cl)InTPPorph and PyC$_{60}$ are approximately an order of magnitude higher than those of the dyads based on (Cl)InTPPorph(2-OMe)$_4$ and Py$_3$C$_{60}$. Hence, the OMe group in porphyrin and the pyridin-2-yl substituents in Py$_3$C$_{60}$ cause a decrease in the probability of the formation of porphyrin—fullerene coordination dyads. The presence of two pyridin-2-yl substituents in Py$_3$C$_{60}$ reduces the basicity of the nitrogen atom in the third pyridyl moiety (pyridin-2-yl), which is involved in the coordination to fullerene. Indium(III) porphyrin complexes were shown to be promising for the development of photoconverters due to high affinity for fullerene-containing organic bases and the higher molar absorption coefficient in the near UV-Vis region ((Cl)InTPPorph, logε = 4.98 with a maximum at λ = 420 nm in CHCl$_3$).

Macroheterocyclic complexes of Porph/Pc with d-metals also have the unique ability to coordinate different molecules, in particular fullerenes, by forming donor-acceptor dyads and triads with promising optical and photoelectric properties and have intramolecular photoinduced electron transfer properties. For example, ruthenium(II) Porph/Pc can be used to control the geometry and stoichiometry of donor-acceptor systems. The presence of the strongly bound carbonyl ligand in one of the two axial Ru^{II} coordination sites facilitates the coordination of another ligand, in particular fulleropyrrolidine, on the opposite side of the macrocycle.[42,144] Donor-acceptor

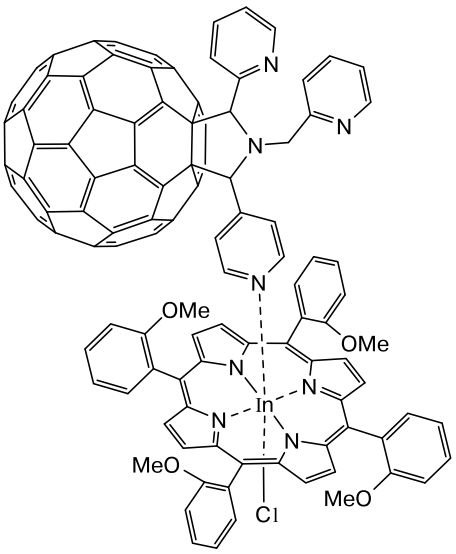

50

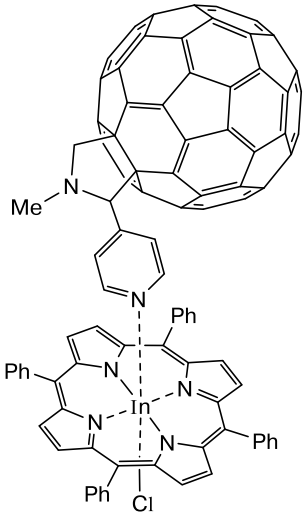

51

Compound	β/L mol^{-1}
50	$2.3 \cdot 10^3$
51	$6.9 \cdot 10^4$

complexes based on ruthenium(II) carbonyl tetraphenylporphyrinate and fullero[60]pyrrolidine derivatives functionalized with the pyridine ring and a hydrophilic chain (**52**—**54**) were synthesized[144] as a model for the investigation of the electron transfer process and in order to prepare Langmuir—Blodgett (LB) films. The structures of these complexes were confirmed by ^{1}H and ^{13}C NMR and UV-Vis spectroscopy and mass spectrometry. The cyclic voltammetry study of dyad **52** showed that several electron transfers occur during the scan, and the dyad displayed a higher stability in terms of reduced and oxidized states. To circumvent the annihilation problem, dyad **53** was spread on a quartz slide as a 1 : 20 mixture with arachidic acid to form LB films.[144] In the monolayers that formed, the dyad molecules are rather spaced apart, thereby ruling out their electronic communication. Photophysical studies (time-resolved transient absorption spectrophotometry) demonstrated that electron transfer occurs in the solid film with a lifetime of the radical ion pair of 2.2 ms.

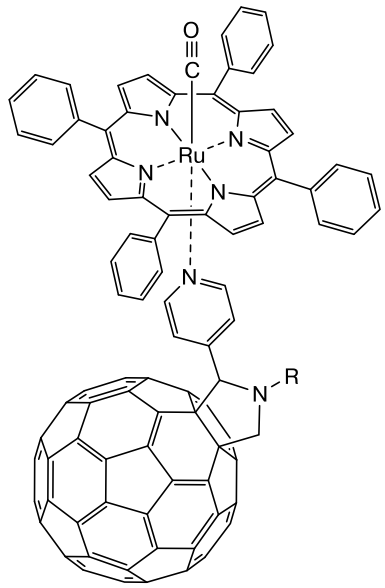

52—55

R = Me (**52**), 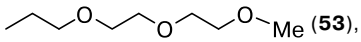 (**53**),

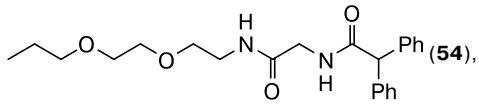 (**54**),

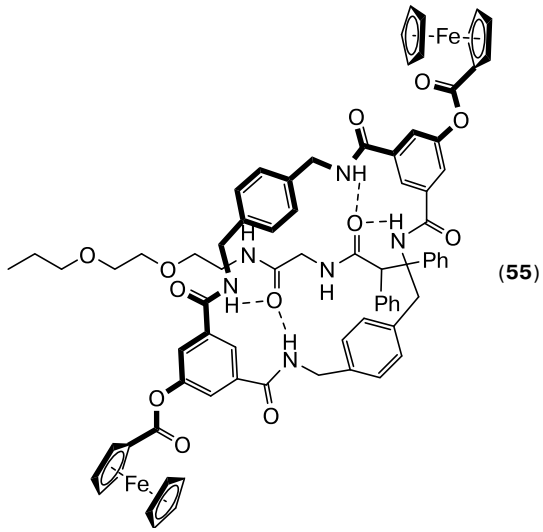 (**55**)

Mateo-Alonso *et al.*[145] went further and synthesized triad **55**. This triad is based on (CO)RuTPP and pyridyl-substituted fullerene (electron acceptor) containing two ferrocene (Fc) electron donors coupled by hydrogen bonds in a rotaxane fashion. The authors suggested that this

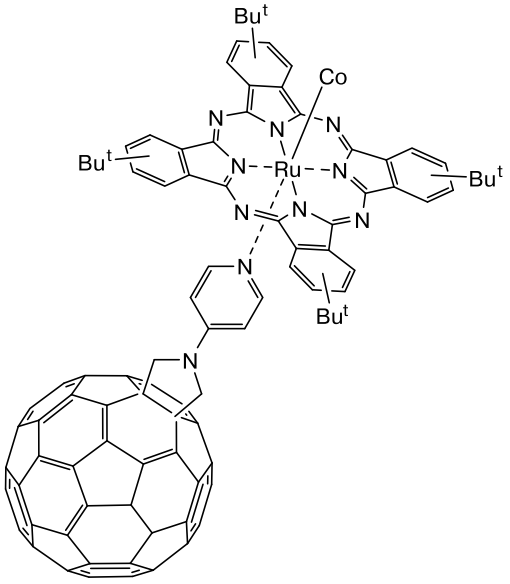

56

combination of entities in the system promotes a unidirectional cascade of two consecutive charge transfer reactions between the three units. The formation of triad **55** was monitored by electronic and NMR spectroscopy. The photophysical behavior of the triad and its components was studied in detail by time-resolved transient absorption spectrophotometry in CH_2Cl_2. The excitation of (CO)RuTPP induces electron transfer to C_{60} to form the (CO)RuTPP$^{\bullet+}$—$C_{60}^{\bullet-}$ radical ion pair. The subsequent charge shift gives rise to the $C_{60}^{\bullet-}$—$Fc^{\bullet+}$ pair with a lifetime of 26 ns. A comparison of the lifetimes of the (CO)RuTPP$^{\bullet+}$—$C_{60}^{\bullet-}$ radical ion pair in dyad **54** (2200 ps) and triad **55** (895 ps) showed that it is 2.5 times shorter in the triad than that in the dyad, which is indicative of an accelerated decay due to the charge transfer shift in triad **55**. However, the lifetime of the final charge transfer product in the triad is longer than that in the dyad and remains persistent for 3.0 ns, *i.e.*, exceeds the 3.0 ns time window of the available apparatus. These data show the prospects of investigations of supramolecular systems having donor-acceptor geometry.

Donor-acceptor complexes **56**—**58** were synthesized[42] in order to evaluate the effect of the donor to acceptor ratio on the chemical, electrochemical, and photophysical properties of supramolecular systems. It was found that the electron distribution in the ground state of donor-acceptor systems **56**—**58** strongly depends on the presence of a powerful π-acceptor carbonyl group in their structures. By contrast, in the excited state, the behavior of these

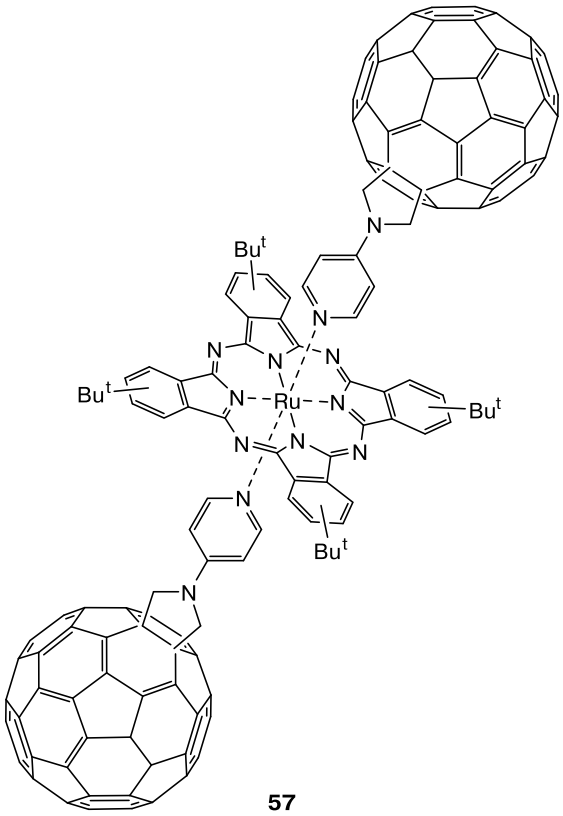

57

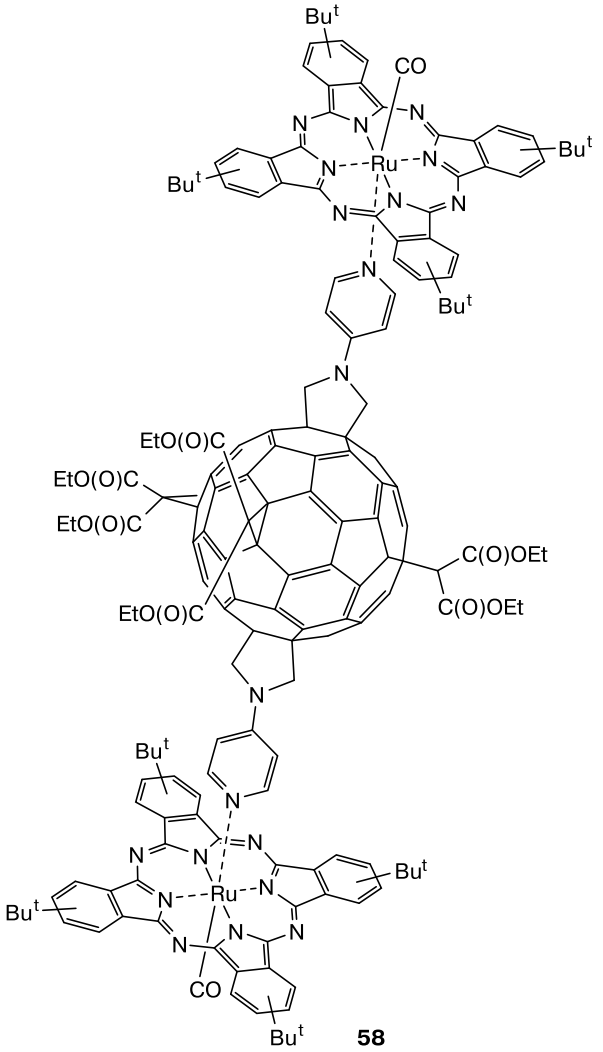

58

systems significantly depends on the number of coordinated fullerene molecules. Therefore, it was shown that donor-acceptor systems based on RuPc and pyridyl-substituted fullerenes are universal platforms for the fine tuning of the results and the dynamics of charge transfer processes. The use of RuPc instead of the corresponding ZnPc with a high-lying triplet excited state made it possible to suppress energy loss and undesirable charge recombination and achieve long lifetimes of the radical ion pairs up to hundreds of nanoseconds for systems **56** and **57**. It should be noted that for system **58**, despite a high energy of the radical ion pair (the reduction potential is shifted to cathodic values), the energy level of the triplet excited state of RuPc is insufficiently high and provides rapid deactivation of the radical ion pair state.

The advantages of cobalt porphyrin/phthalocyanine complexes (CoPorph/CoPc) are high chemical, electrochemical, and photochemical stability and high coordination capacity of the central metal atom, promoting the modification of these compounds at the axial position to form thermodynamically stable donor-acceptor systems with fullerenes. This is important in studies of the components used in photovoltaic devices. It was shown that cobalt(II) porphyrin complexes form donor-acceptor triads (**59—64**) with pyrrolidinyl[60]fullerenes, whereas only dyads (**65—68**) are formed with cobalt phthalocyanine.[27—32,146,147]

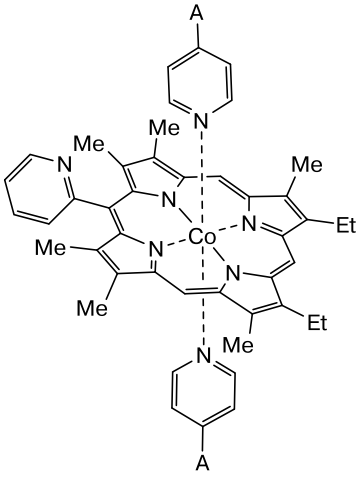

59, 60

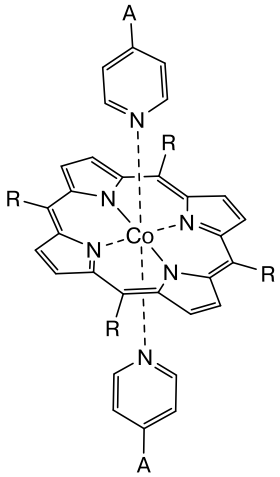

61, 62, 64

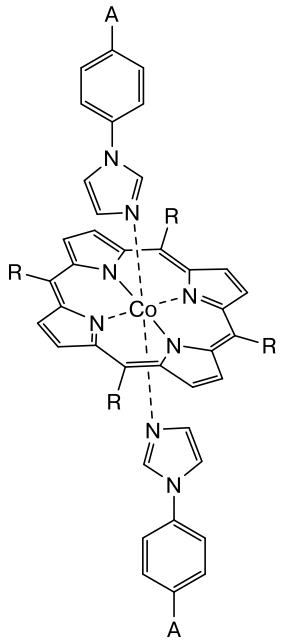

63

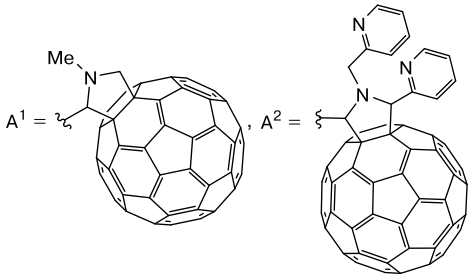

A = A^1 (**59**, **61—64**), A^2 (**60**)

Compound	R	K_1/L mol^{-1}	K_2/L mol^{-1}	$\beta = K_1 \cdot K_2$/L^2 mol^{-2}
59	—	$1.79 \cdot 10^4$	$5.76 \cdot 10^5$	$1.04 \cdot 10^{10}$
60	—	$9.30 \cdot 10^3$	$6.00 \cdot 10^4$	$5.58 \cdot 10^8$
61	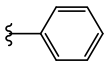	$5.43 \cdot 10^4$	$8.69 \cdot 10^4$	$4.69 \cdot 10^9$
62	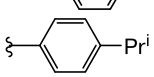	$1.59 \cdot 10^4$	$2.02 \cdot 10^5$	$2.21 \cdot 10^9$
63	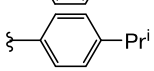	$3.29 \cdot 10^4$	$6.23 \cdot 10^4$	$2.05 \cdot 10^9$
64	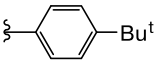	$1.04 \cdot 10^4$	$1.21 \cdot 10^6$	$1.34 \cdot 10^{10}$

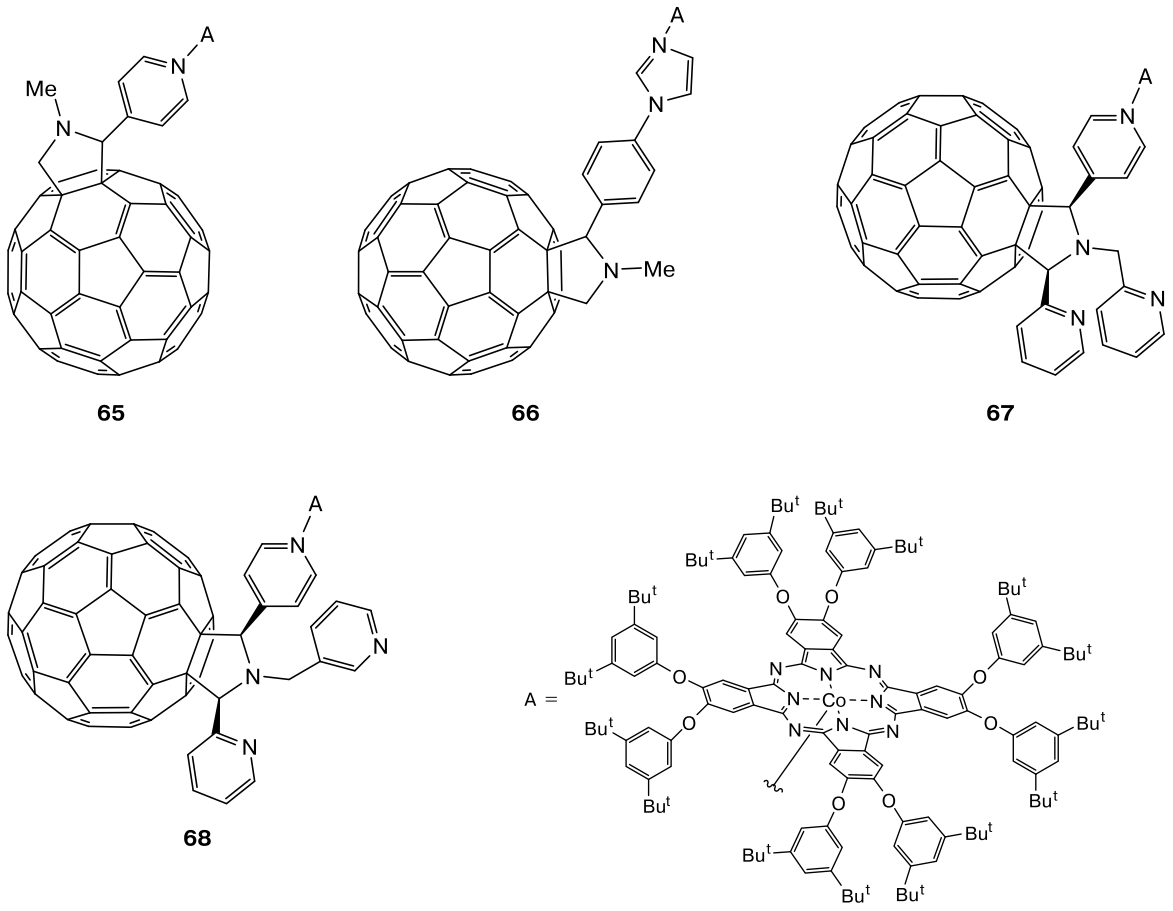

65 **66** **67**

68

A =

β = 5.62 • 10^5 (**65**), 6.60 • 10^5 (**66**), 1.84 • 10^5 L mol^{-1} (**67**)

The reactions of CoPorph with pyridyl-substituted pyrrolidinyl[60]fullerenes were studied by spectrophotometric methods, which enabled the accurate determination of the thermodynamic and kinetic parameters of the process and the observation of the spectral difference between the five- and six-coordinate metalloporphyrin complexes. The investigation of the reactions of CoPorph (Porph is 5,10,15,20-tetraphenylporphyrin, 5,10,15,20-tetra(4-isopropylphenyl)porphyrin, 5,10,15,20-tetra(4-*tert*-butylphenyl)porphyrin, and 2,3,7,8,12,18-hexamethyl-13,17-diethyl-5-(2-pyridyl)porphyrin) with PyC_{60}/ImC_{60}/Py_3C_{60} showed the occurrence of two equilibria. The first fullerene molecule is coordinated immediately after the mixing of the reagents, whereas the coordination of the second C_{60} molecule takes place at a measurable rate. Both equilibria were quantitatively characterized using the time-dependent spectrophotometric titration.* An analysis of the numerical values of the equilibrium constants in the first (K_1) and second (K_2) steps and the total stability constant (β_{tot}, $\beta_{tot} = K_1 \cdot K_2$) of the triads showed that the stability of the supramolecular systems depends on the nature of the substituents at the macrocycle and fullero-[60]pyrrolidine. Donor-acceptor triads **59** and **64** proved to be the most stable. Apparently, the presence of electron-donating alkyl substituents in the porphyrin ligand stabilizes these supramolecular systems. The structures of the synthesized dyads and triads were confirmed by IR and ^{1}H NMR spectroscopy. The geometric parameters of triad **59** were determined by density functional theory quantum chemical calculations (DFT, B3LYP-D3/6-31G (d,p)). According to these calculations, the pyridine rings of PyC_{60} in triad **59** are perpendicular to the plane of the porphyrin, and the Co—$N_{PyC_{60}}$ distances are 2.263 and 2.288 Å.[28] The electron density of the HOMO and LUMO is spread over the porphyrin and fullerene entities, respectively. The experimental data, the results quantum chemical calculations, photochemical measurements, and cyclic voltammetry features suggest the occurrence of the efficient photoinduced electron transfer in triad **59**. The CV study of the resulting macroheterocyclic complexes showed changes in the redox potentials of the individual components, which is evidence of the interaction between these components.

The reaction of cobalt(II) octakis(3,5-di-*tert*-butylphenoxy)phthalocyaninate with fullero[60]pyrrolidines affords

* Processing of the results of the spectrophotometric titration at $\tau = 0$ and $\tau = \infty$ after the completion of the slow reaction for all compositions of the mixture.

donor-acceptor dyads **65—68** rather than triads. This is apparently due to the steric factor associated with the presence of the highly branched system of substituents at the periphery of the macrocycle. An analysis of the stability constants (β) of these dyads showed that dyad **66** is the most stable one, This is apparently attributed to the structural features of pyrrolidinofullerene, such as the presence of the imidazole group more basic compared to the pyridyl moiety. The photoinduced electron transfer in dyad **66** was demonstrated using time-resolved transient absorption spectroscopy, and the rates of charge separation ($1.4 \cdot 10^{13}$ s^{-1}) and charge recombination ($4.0 \cdot 10^{10}$ s^{-1}) were determined for the $CoPc^{\bullet+}$—$ImC_{60}^{\bullet-}$ radical ion pair.[147]

The modification of a titanium dioxide electrode with natural oxide film (NOF) by the synthesized donor-acceptor systems based on CoPorph/CoPc allowed the determination of their photoelectrochemical properties. The photocurrent density (j_{ph}) and the IPCE (the monochromatic analog of the external quantum efficiency) were determined in a Ti|film|0.5 mol L^{-1} Na_2SO_4|Pt short-circuited electrochemical cell upon irradiation of the samples by monochromatic light at λ = 365 nm (Table 5). An analysis of these values showed that the photocurrent and IPCE of the TiO_2 electrode modified with fullerene-containing Porph/Pc systems are 2—3-fold larger compared to the corresponding values of the individual components of the donor-acceptor systems. The largest values of j_{ph} and IPCE were observed for the films modified with triad **59**.

Other representatives of macroheterocyclic d-metal complexes are manganese(III) porphyrinates/phthalocyaninates (MnPorph/MnPc). The reactions of these complexes with pyridyl-substituted fullerenes afford exclusively donor-acceptor dyads (**69—76**). It was noted that the nature of the tetrapyrrole macrocycle has no effect on the composition of the products but influences the time of the synthesis of the fullerene–based manganese(III) macroheterocyclic complex and the stoichiometry of the reaction. Thus, the formation of dyad **69** based on (Cl)MnOEP and PyC_{60} occurs within 5 days,[148] whereas the formation of dyads based on manganese(III) (octakis(4-*tert*-butylphenyl))tetraazaporphyrinate acetate (**70**, **71**)[149,150] and manganese(III) (octakis(3,5-fi-*tert*-butylphenoxy))phthalocyaninate acetate (**72—74**)[147,151,152] requires 10—60 min. In the case of (Cl)MnOEP, the addition of PyC_{60} is a slow one-step irreversible process, whereas in the case of manganese(III) tetraazaporphyrin complexes, the reaction occurs in two steps. The latter process involves the rapid irreversible coordination of fullerene at the manganese atom in the macrocycle and the subsequent irreversible displacement of the acetate ion from the coordination dyad. The displacement rate constant is inversely dependent on the fullerene concentration in a first-order manner. According to the spectrophotometric measurements, the formation of dyads **72—76** in the case of MnPc is described as a two-step process with a rapidly established equilibrium between the starting compounds and the donor-acceptor complex followed by the slow displacement of the acetate

Table 5. Photocurrent density (j_{ph}) and the incident photon-to-current efficiency (IPCE) for the Ti|film|0.5 mol L^{-1} Na_2SO_4|Pt system upon irradiation of the samples by monochromatic light at λ = 365 nm[a]

No.	Titanium electrode with NOF	j_{ph}/μA cm^{-2}	IPCE (%)	Ref.
1	Natural oxide film	0	0	—
2	PyC_{60} ($C_{PyC_{60}} = 1.5 \cdot 10^{-4}$)	96.58	23.27	
	CoPorph ($C_{CoPorph} = 1.8 \cdot 10^{-5}$)[b]	116.69	28.11	
	59 ($C_{CoPorph} = 1.8 \cdot 10^{-5}$, $C_{PyC_{60}} = 1.5 \cdot 10^{-4}$)	287.04	69.16	28
3	PyC_{60} ($C_{PyC_{60}} = 2.7 \cdot 10^{-5}$)	78.95	19.02	
	CoTPPorph ($C_{CoTPPorph} = 3.5 \cdot 10^{-6}$)	77.53	18.68	
	61 ($C_{CoTPPorph} = 3.5 \cdot 10^{-6}$, $C_{PyC_{60}} = 2.7 \cdot 10^{-5}$)	166.91	40.22	32
4	PyC_{60} ($C_{PyC_{60}} = 2.7 \cdot 10^{-5}$)	78.95	19.02	
	CoPorph ($C_{CoPorph} = 4.2 \cdot 10^{-6}$)[c]	85.80	20.67	
	64 ($C_{CoPorph} = 4.2 \cdot 10^{-6}$, $C_{PyC_{60}} = 2.7 \cdot 10^{-5}$)	175.05	42.18	31
5	PyC_{60} ($C_{PyC_{60}} = 1.5 \cdot 10^{-4}$)	96.58	23.27	
	CoPc ($C_{CoPc} = 5.3 \cdot 10^{-5}$)	98.31	23.69	
	65 ($C_{CoPc} = 5.3 \cdot 10^{-5}$, $C_{PyC_{60}} = 1.3 \cdot 10^{-4}$)	233.50	56.26	29
6	ImC_{60} ($C_{ImC_{60}} = 1.4 \cdot 10^{-4}$)	98.23	23.67	
	CoPc ($C_{CoPc} = 5.3 \cdot 10^{-5}$)	98.31	23.69	
	66 ($C_{CoPc} = 5.3 \cdot 10^{-5}$, $C_{ImC_{60}} = 1.3 \cdot 10^{-4}$)	244.32	58.87	147

[a] *C* are the concentrations of the components, mol L^{-1}.
[b] CoPorph is cobalt(II) 2,3,7,8,12,18-hexamethyl-13,17-diethyl-5-(2-pyridyl)porphyrinate.
[c] CoPorph is cobalt(II) 5,10,15,20-tetra(4-*tert*-butylphenyl)porphyrinate.

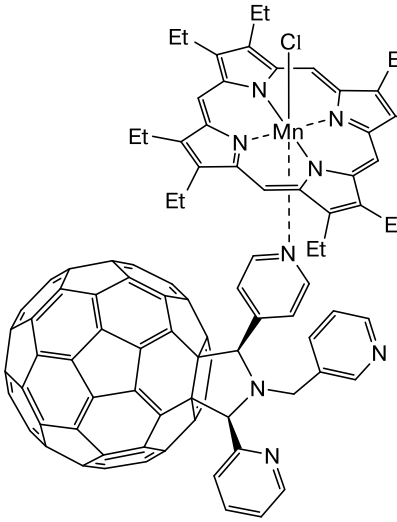

69

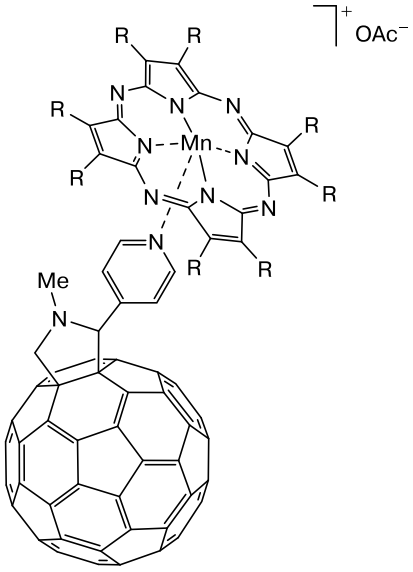

70, 72, 75, 76

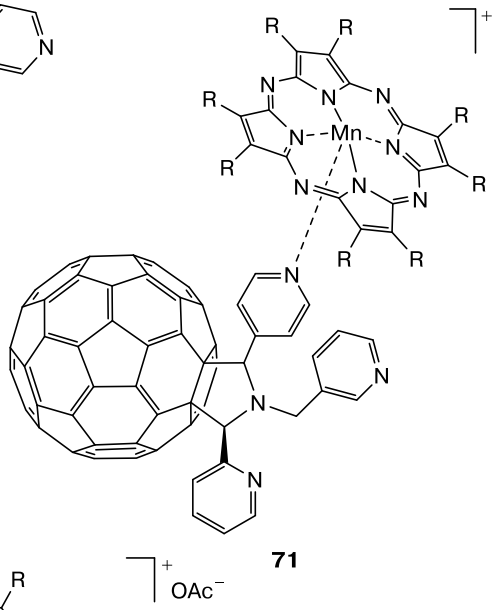

71

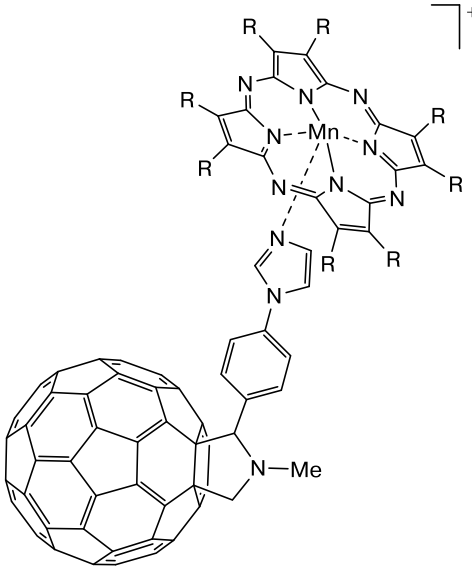

73

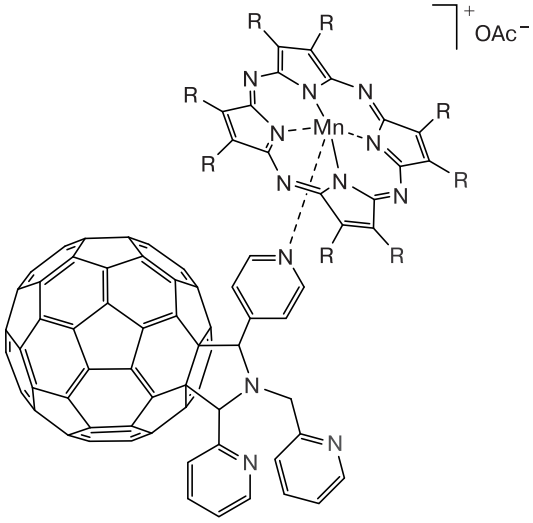

74

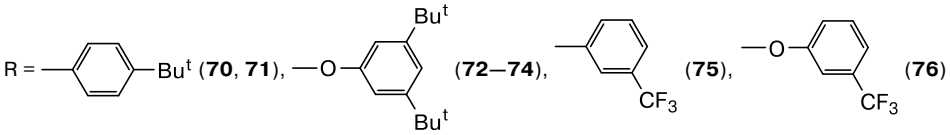

Dyad	β/L mol^{-1}	Dyad	β/L mol^{-1}
72	$2.4 \cdot 10^4$	**75**	$2.3 \cdot 10^3$
73	$3.8 \cdot 10^4$	**76**	$3.8 \cdot 10^4$
74	$1.7 \cdot 10^4$		

ion to the outer coordination sphere. The rate of the latter reaction was independent of the PyC_{60} concentration. The IR spectroscopic study of dyads **70—76** confirmed the formation of cationic donor-acceptor complexes. In the spectra of these compounds, the frequency difference between two stretching vibrations ν_{as}(O—C—O) and ν_s(O—C—O) was less than 225 cm^{-1}, which is indicative of the ionic binding mode of the acetate anion.

It was shown[64] that the fluorine-containing substituents in the macrocyclic ligand can terminate the electronic coupling in the phthalocyanine—fullerene dyad and prevent the intramolecular electron transfer from Pc to fullerene, whereas its nonfluorinated analog shows intramolecular photoinduced electron transfer. In the case of dyads **75** and **76** containing 3-fluoromethylphenyl- and 3-fluoromethylphenoxy groups, respectively, the photoinduced electron transfer was confirmed by quantum chemical calculations (the electron density distribution of HOMO in the porphyrin entity and LUMO in the fullerene entity) and by fluorescence spectroscopy (based on fluorescence quenching of MnPc upon the formation of the donor-acceptor system).[152] In dyads **72** and **73**, this transfer is evidenced by the cyclic voltammetry data (based on the shift of the redox potentials of individual components upon the formation of dyads) and femtosecond transient absorption spectroscopy (the charge separation and recombination rates are $1.25 \cdot 10^{13}$ and $1.0 \cdot 10^9$ s^{-1}, respectively, for dyad **73**).[147]

The photocurrent density and the incident photon-to-current efficiency (IPCE, λ = 365 nm), measured using a titanium dioxide electrode modified with donor-acceptor systems **70**, **72**, and **73**, are given in Table 6. It is seen that the dyad films, rather than individual components, have high photoelectrochemical characteristics. Hence, supramolecular systems are promising for the preparation of components for photovoltaic devices.

Researchers paid attention to porphyrin complexes with metals, which have a formal charge higher than three due to a high coordination capacity along the axial direction. This improves the coordination of pyrrolidinyl-substituted fullerene to form porphyrin—fullerene systems of different orders. Thus, porphyrin—fullerene dyad **77** and triad **78** based on molybdenum(V) hydroxo(5,10,15,20-tetraphenylporphyrinate) (Mo(O)(OH)TPP) were synthesized.[37,38] The equilibria and rate constants in the course of the synthesis were quantitatively characterized. According to the spectrophotometric study, the reaction between Mo(O)(OH)TPP and fullero[60]pyrrolidine involves two steps: the rapid establishment of the equilibrium between the starting compounds and the 1 : 1 donor-acceptor complex and the subsequent slow irreversible dis-

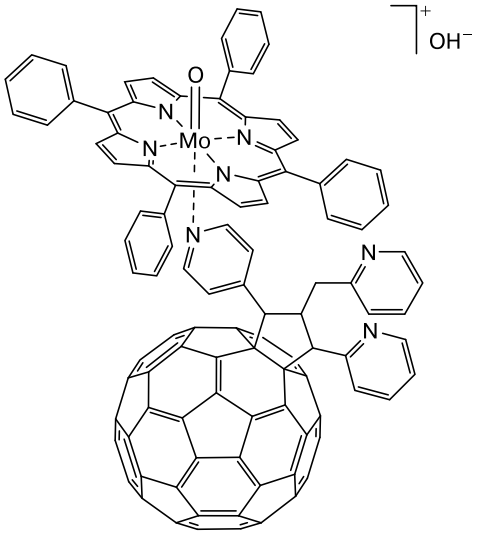

77

($\beta = 1.97 \cdot 10^4$ L mol^{-1})

Table 6. Photocurrent density (j_{ph}) and IPCE (λ = 365 nm) for the Ti|film|0.5 mol L^{-1} Na_2SO_4|Pt system[a]

No.	Titanium electrode with NOF	j_{ph}/μA cm^{-2}	IPCE (%)
1	NOF	0	0
2	PyC_{60} ($C_{PyC_{60}} = 1.5 \cdot 10^{-4}$)	96.58	23.27
	MnPorph(AcO) ($C_{MnPorph(AcO)} = 2.9 \cdot 10^{-5}$)[b]	92.82	22.36
	70 ($C_{MnPorph(AcO)} = 2.9 \cdot 10^{-5}$, $C_{PyC_{60}} = 1.5 \cdot 10^{-4}$)	203.91	49.13
3	PyC_{60} ($C_{PyC_{60}} = 1.5 \cdot 10^{-4}$)	96.58	23.27
	MnPc(AcO) ($C_{MnPc(AcO)} = 3.0 \cdot 10^{-6}$)	109.8	26.46
	72 ($C_{MnPc(AcO)} = 3.0 \cdot 10^{-6}$, $C_{PyC_{60}} = 1.5 \cdot 10^{-4}$)	239.63	57.74
4	ImC_{60} ($C_{ImC_{60}} = 1.4 \cdot 10^{-4}$)	98.23	23.67
	MnPc(AcO) ($C_{MnPc(AcO)} = 4.0 \cdot 10^{-6}$)	109.80	26.46
	73 ($C_{MnPc(AcO)} = 4.0 \cdot 10^{-6}$, $C_{ImC_{60}} = 1.4 \cdot 10^{-4}$)	252.74	60.90

[a] The concentrations of the components (C), mol L^{-1}.

[b] MnPorph(AcO) is manganese(III) (octakis(4-*tert*-butylphenyl))tetraazaporphyrin acetate.

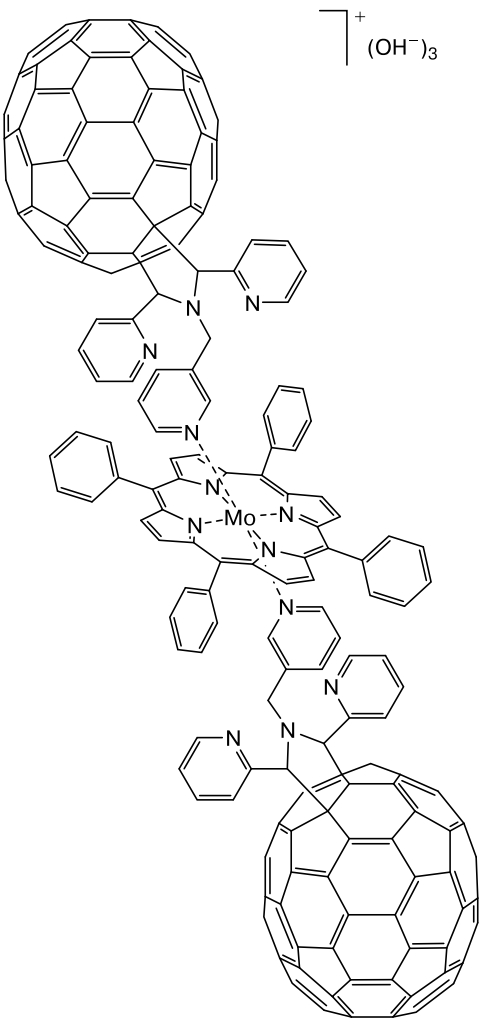

78

(β_{tot} = 2.94 · 10^7 L^2 mol^{-2})

placement of the hydroxo ligand OH^- to the outer coordination sphere to form outer-sphere cationic complex **77**.

The reaction of Mo(O)(OH)TPP with pyridyl-substituted pyrrolidinyl[70]fullerene also occurs in two steps to form 1 : 2 outer-sphere cationic complex **78**. The structures of the synthesized compounds were confirmed by UV-Vis and IR spectroscopy, and the occurrence of photoinduced electron transfer in these systems was proved by fluorescence spectroscopy. The addition of pyrrolidinylfullerene to Mo(O)(OH)TPP in toluene leads to a decrease in the fluorescence intensity of the molybdenum(v) porphyrin complex by ≥50%, which can be considered as evidence of the photoinduced electron transfer in the porphyrin—fullerene triad, like the primary charge separation in a photosynthetic antenna.

Porphyrin—fullerene systems based on rhenium(v) and niobium(v) complexes were synthesized and characterized by UV-Vis and fluorescence spectroscopy.[40,41,153] These studies confirmed the formation of donor-acceptor dyads in CH_2Cl_2 in the case of Re(O)(Cl)Porph (Porph is 5,15-bis-(4-methoxyphenyl)-3,7,13,17-tetramethyl-2,8,12,18-tetraethylporphyrin) and Re(O)(OPh)Porph (Porph is 5-monophenyl-2,3,7,8,12,13,17,18-octaethylporphyrin) and in toluene in the case of $(Cl)_3$NbPorph (Porph is 5,10,15,20-tetra(4-*tert*-butylphenyl)porphyrin). Despite insignificant changes in the UV-Vis spectra of rhenium(v) porphyrins in the presence of pyridyl-substituted pyrrolidinyl[60]fullerene, the formation of the donor-acceptor complex and the charge redistribution in this complex are evidenced by a significant decrease in the fluorescence intensity of free fullerene compared to the substituted fullerene linked to metalloporphyrin.[41] In the case of $(Cl)_3$NbPorph in the presence of PyC_{60}, significant changes in the UV-Vis spectra are observed (the bathochromic shift of the Soret band by 14 nm). Unlike rhenium

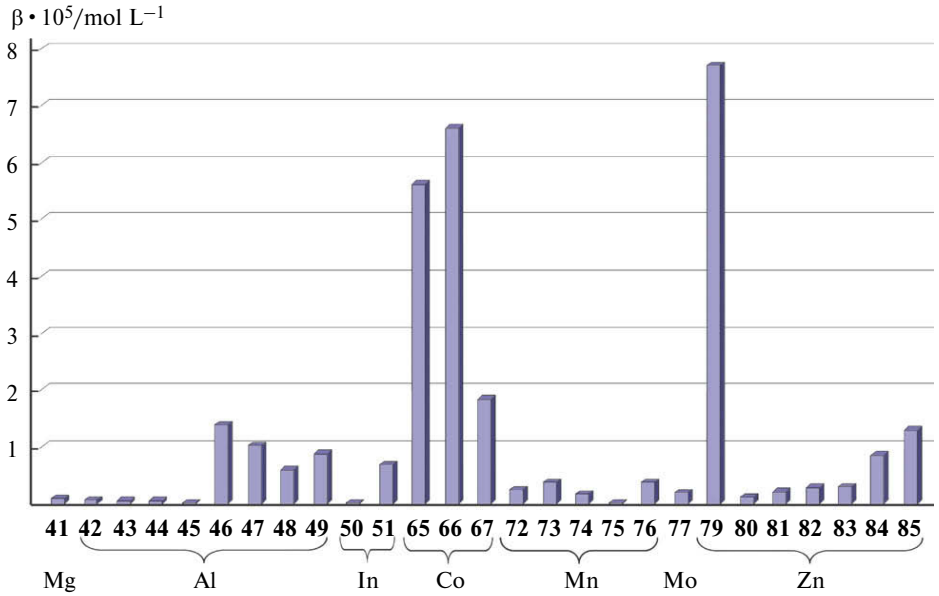

Fig. 2. Diagram of stability of donor-acceptor metalloporphyrin—fullerene and metallophthalocyanine—fullerene dyads.

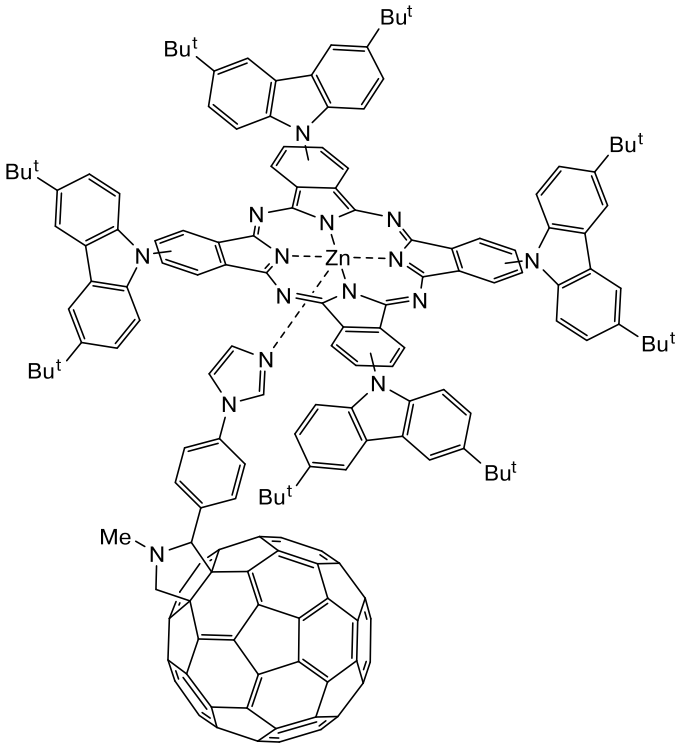

79

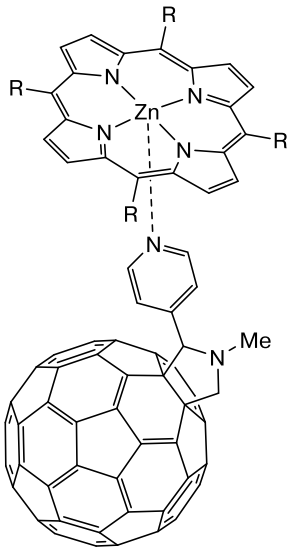

80, 82

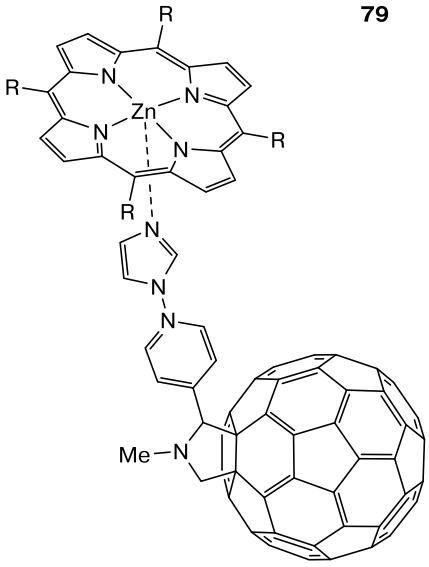

81, 83

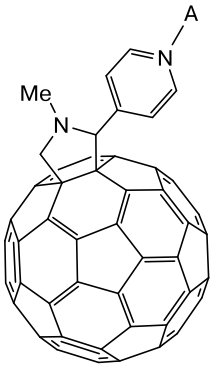

84

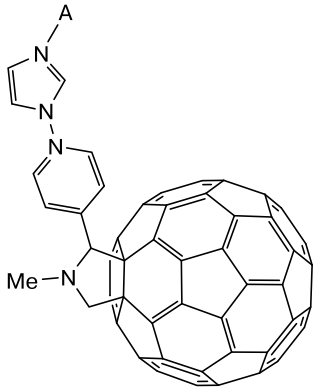

85

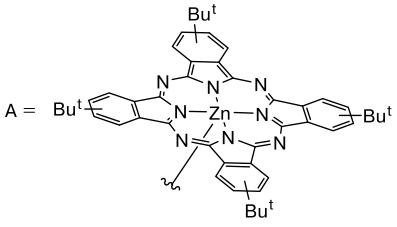

Table 7. Stability constants of supramolecular systems (**79—85**) based on zinc porphyrins/phthalocyanines[154—156]

System	R	β/L mol^{-1}
79	—	$7.70 \cdot 10^5$
80	C_6H_5	$1.20 \cdot 10^4$
81	C_6H_5	$2.10 \cdot 10^4$
82	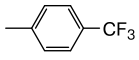	$2.90 \cdot 10^4$
83	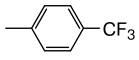	$3.00 \cdot 10^4$
84	—	$8.60 \cdot 10^4$
85	—	$1.30 \cdot 10^5$

porphyrinates, $(Cl)_3$NbPorph shows fluorescence properties, making it possible to detect electron transfer based on the fluorescence quenching of metalloporphyrin upon the formation of a donor-acceptor system.

An analysis of supramolecular systems based on fullerenes and MPorph/MPc complexes with a central metal cation other than zinc demonstrated that the stability can be predicted and the composition of the resulting donor-acceptor systems can be changed by varying the central metal in the plane of the macrocycle (Fig. 2). The stability constants of fullerene dyads based on zinc complexes **79**—**85** are given in Table 7.

3. Gold(III) porphyrins as acceptor ligands in photoinduced charge-transfer systems

Gold(III) porphyrin complexes hold a special place among d-metal macroheterocyclic complexes. These complexes form covalent and donor-acceptor systems and act as electron acceptors. In these systems, zinc porphyrinates/phthalocyaninates are utilized as electron donors. These structures are poorly characterized and provide a new approach to the preparation of systems with photoinduced electron transfer. First systems of this type, in which ZnPorph as an electron donor and AuPorph as an electron acceptor are covalently linked through a 2,10-diphenyl-1,10-phenanthroline spacer, were synthesized in the early 1990s.[157,158] It was shown that the selective excitation of any porphyrin in these systems induces rapid electron transfer from zinc porphyrinate to gold porphyrinate. The electron transfer rate correlates well with the exothermicity of the reaction and the temperature, but weakly correlates with the polarity of the solvent because of the limited applicability of the dielectric continuum model to this system and the solvent-induced changes in the redox potentials.[157] The electronic structure of the spacer or the bridging chromophore between the porphyrin entities also influences the electronic coupling between the donor and the acceptor. Systems based on zinc and gold porphyrins covalently linked by bridging chromophores with different structures were characterized.[159] Three of these systems (**86**—**88**) are fully π-conjugated, and in one system (**89**) the conjugation is broken. These systems showed rapid photoinduced electron transfer at the intercenter distance *r*(Zn—Au) of 25 Å. When the conjugation in the bridge is broken, the rate of fluorescence quenching of the donor sharply decreases, and the quenching of the residual fluorescence corresponds to the expected singlet-singlet energy transfer. According to the experimental data and the results of quantum chemical calculations, the interaction between the donor and the acceptor depends on the bridging chromophore. The investigation showed that there is an inverse relationship with the energy gap between the excited states of the donor and the bridge.

The effect of the chemical structure of the spacer on the physicochemical and electrochemical properties in related systems has been extensively investigated.[160—162] New conjugates with spacers of different lengths (**90**—**92**) showing photoinduced electron transfer were synthesized.[161] The distance between the centers of metalloporphyrins in these dyads vary from 32 to 45 Å. The spectroscopic and electrochemical studies demonstrated strong electronic coupling.

According to femtosecond fluorescence spectroscopy, the dyad with a long spacer **92** has the longest lifetimes (40 and 390 ps in dichloromethane and toluene, respectively). For other dyads in different solvents, the fluorescence lifetime varies from 3 to 7 ps. It is worth noting that the lifetime for the corresponding zinc complexes with spacers **90**—**92** is 1600—1800 ps regardless of the solvent.

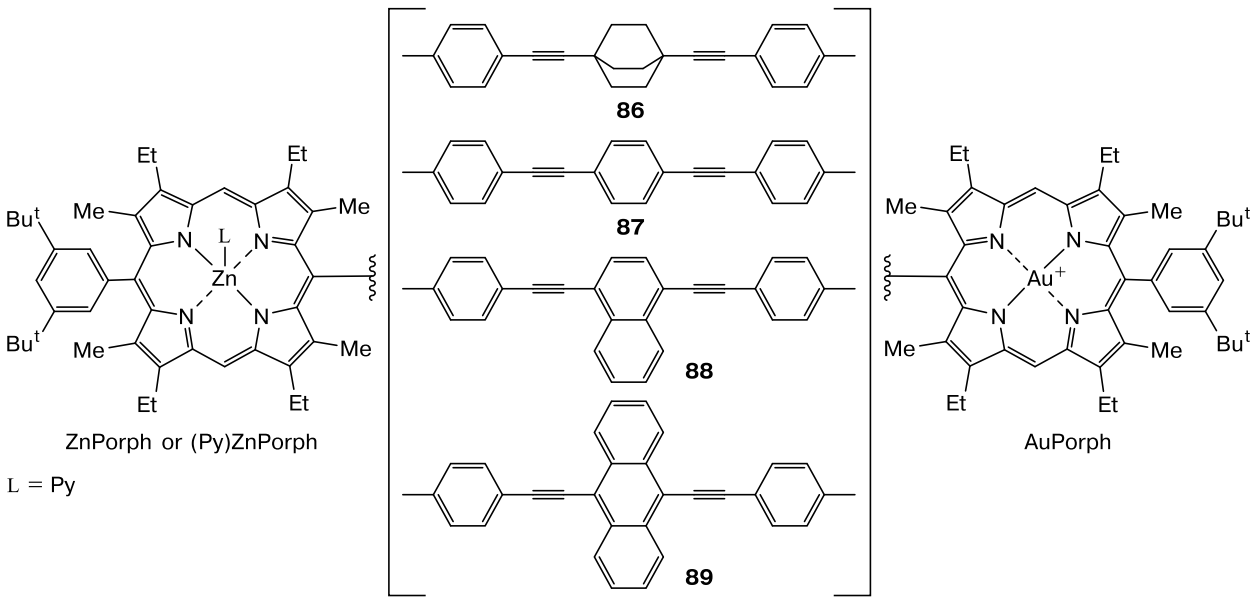

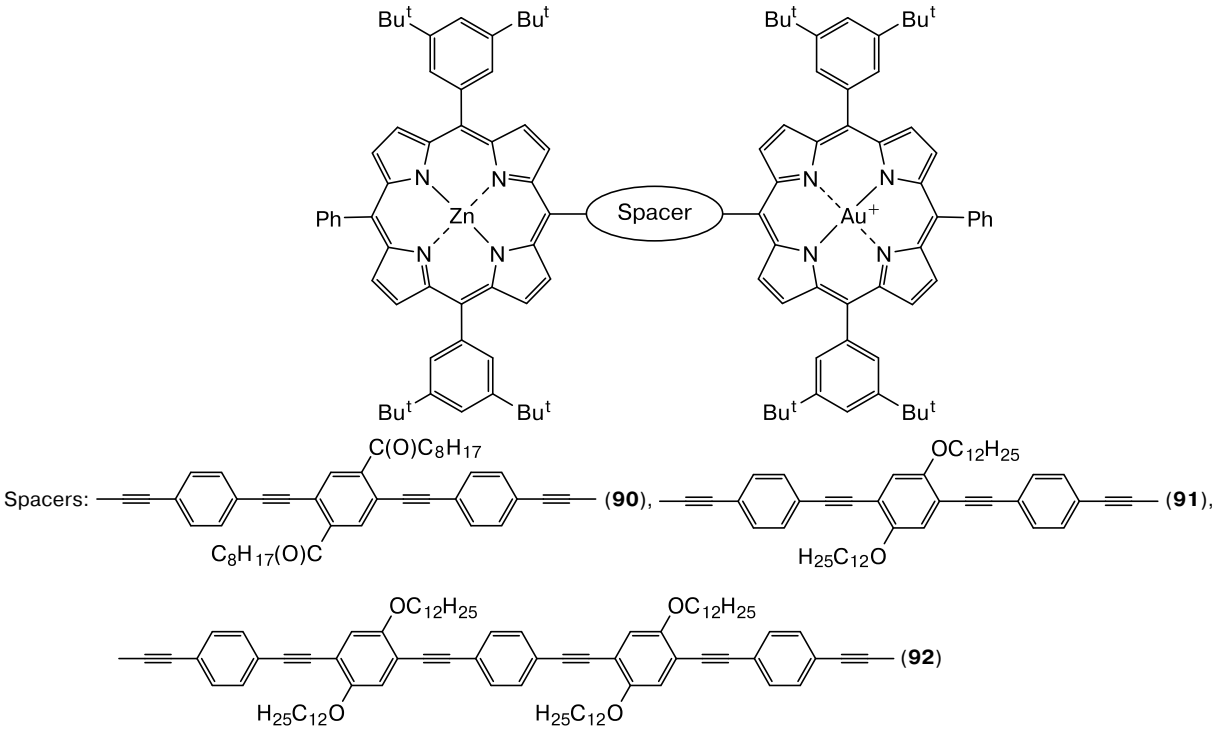

The investigation of electron transfer in these systems by femtosecond transient absorption spectroscopy demonstrated that the formation of the charge-separated state in dichloromethane is a spontaneous process that occurs through the electron transfer (ET) and hole transfer (HT). It was noted[161] that the back electron transfer (BET) occurs in toluene, giving rise to the triplet state of zinc(II) porphyrin (^{3}ZnPorph).* The parameters characterizing these processes are given in Table 8.

Therefore, the dependence of the charge transfer mechanisms on the polarity of the medium provides an approach to the fabrication of desired products and also may help in developing new efficient strategies for the synthesis of porphyrin systems exhibiting long-range electron transfer, with potential applications in molecular electronics and solar energy conversion.

The synthesis of dyad **93** based on zinc and gold porphyrinates by the Sonogashira reaction[163] was reported in the study.[164] The electrochemical studies of this compound showed that it is characterized by strong electronic coupling in the ground state, as evidenced by the redox potential shifts and the appearance of the charge transfer band. The lifetimes of the charge-separated states depending on the solvent polarity were determined by studying the electron transfer process using time-resolved absorption spectroscopy. These lifetimes were 200 ps (in DMF), 1 ns (in CH_2Cl_2), and 4 ns (in toluene).

Heteronuclear Porph/Pc systems, in which gold porphyrinate acts as an electron acceptor, were synthesized *via* the axial binding.[165—167] As in the case of porphyrin—

* The superscript 3 indicates the triplet state.

Table 8. Times (τ) for charge transfer processes in different solvents

Spacer	Solvent	Excitation of ZnPorph in the dyad		Excitation of AuPorph in the dyad	
		τ_{ET}/ps	τ_{BET}/ps	τ_{HT}/ps	τ_{BET}/ps
90	CH_2Cl_2	2	80	2	170
90	Toluene	8	240	170[a]	—
91	CH_2Cl_2	2	90	Not observed	
91	Toluene	7	130	130[a]	—
92	CH_2Cl_2	85	2100	Not observed	
92	Toluene	370	≈12000	Not observed	

Note. τ_{ET} is the electron transfer time, τ_{BET} is the back electron transfer time, τ_{HT} is the hole transfer time. [a] The times τ for the energy transfer from ^{3}AuPorph$^+$ to ^{3}ZnPorph.

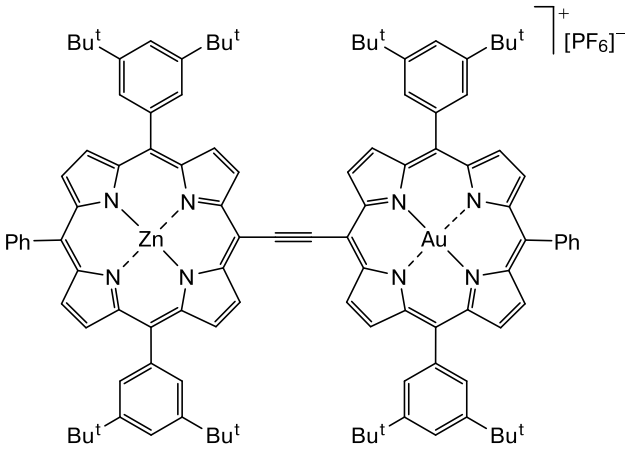

93

fullerene complexes, two axial binding modes can occur in these systems: through a covalent M—O bond[165] and *via* donor-acceptor bonding through M—N coordination.[166,167]

The dyad (**94**) based on aluminum(III) porphyrinate and gold(III) porphyrinate and the triads (**95, 96**) containing these metalloporphyrins with axially coordinated tetrathiafulvalenes (TTF) were synthesized and characterized by diverse spectroscopic and electrochemical methods.[165] An analysis of the fluorescence spectra of dyad **94** demonstrated that fluorescence quenching of aluminum(III) porphyrinate occurs by ~88% with respect to free aluminum(III) porphyrinate, whereas gold(III) porphyrinate does not show fluorescence due to the heavy atom effect. According to the energy diagram and the results of electrochemical measurements, the spontaneous electron transfer can occur from aluminum(III) porphyrinate to gold(III) porphyrinate, as evidenced by strong fluorescence quenching associated with this process. The addition of TTF to a solution of dyad **94** in dichloromethane resulted in the formation of triads **95** and **96**. This was established by the fluorescence titration. An increase in the TTF concentration leads to further fluorescence quenching. The authors explained the quenching mechanism assuming the transfer of positively charged species from aluminum(III) porphyrinate to tetrathiafulvalene. The charge separation and recombination rate constants and the temporal parameters found for these systems and process are given in Table 9.

An analysis of the results confirms the successful preparation of the photosynthetic system by the axial coordination. It is worth noting that the introduction of secondary donors has a positive effect on the charge recombination rate in the triad, significantly decreasing it with respect to the recombination rate in the dyad.

The donor-acceptor bonding between zinc(II) phthalocyaninate and pyridyl-substituted gold(III) porphyrinate (**97**) was reported in the study.[167]

The formation of donor-acceptor complex **97** was studied in *o*-dichlorobenzene by spectrophotometric titr-

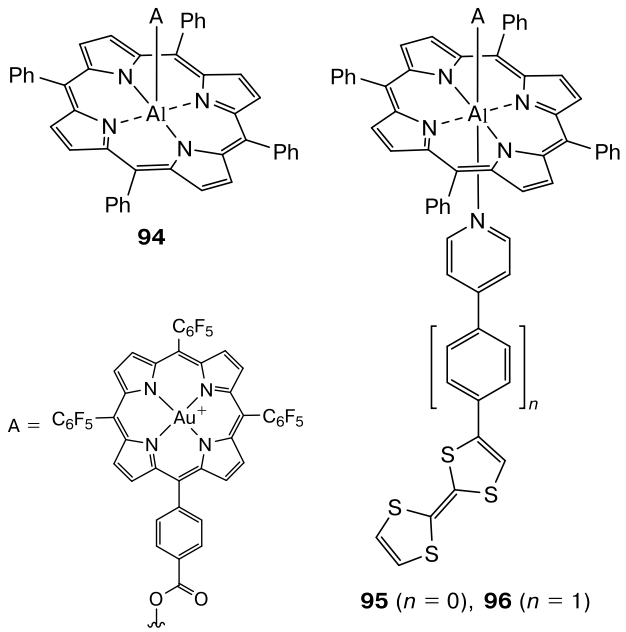

94

95 (n = 0), **96** (n = 1)

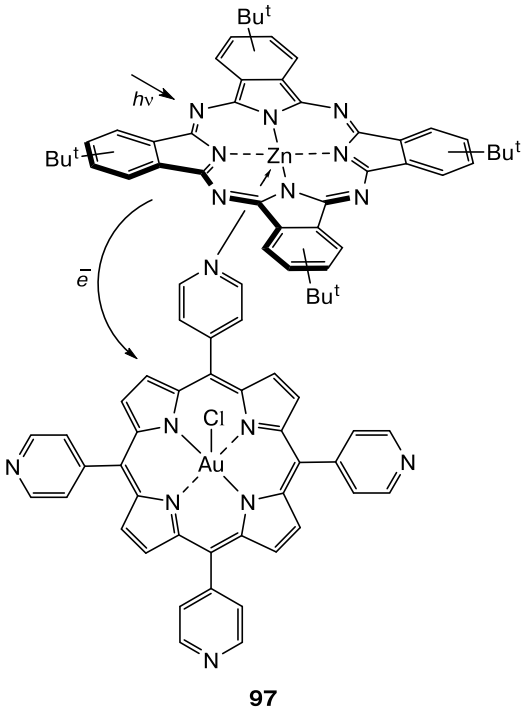

97

Table 9. Time-resolved characteristics of the charge separation and recombination processes for compounds **94—96** in 1,2-dichlorobenzene

Compound	τ_{CS}/ps	k_{CS}/s^{-1}	τ_{CR}/ps	k_{CR}/s^{-1}
94	3.16	$3.12 \cdot 10^{11}$	27.26 (2557)*	$3.67 \cdot 10^{10}$ ($3.91 \cdot 10^{8}$)*
95	15.50	$5.40 \cdot 10^{10}$	1318 (1468)*	$7.59 \cdot 10^{8}$ ($6.81 \cdot 10^{8}$)*
96	61.20	$1.64 \cdot 10^{10}$	1484	$6.74 \cdot 10^{8}$

* The presence of two charge separation rate constants are given for the time-resolved profile described by a biexponential function.

ation with the Benesi—Hildebrand method. The stability constant of the synthesized complex is $2.94 \cdot 10^4$ L mol^{-1}, which is indicative of the formation of the moderately stable complex. It should be noted that this constant can be compared with the stability constants for related systems with pyrrolidinofullerenes.[77] The formation of this supramolecular system leads to fluorescence quenching due to the donor-to-acceptor electron transfer. The stability constant of the system determined by the Stern—Volmer method is $1.20 \cdot 10^5$ L mol^{-1}. The lifetime of the charge-separated state varies from 5.7 to 244 ps. Therefore, this system can be considered as an adequate photosynthetic model.

Conclusion

The review summarizes various strategies for the synthesis of systems with photoinduced charge separation properties based on macroheterocyclic complexes, which are of interest for the design of molecular materials with specified properties. The synthesis of covalently linked porphyrin—fullerene complexes is important for an understanding of the mechanism controlling the photoinduced electron transfer in molecular systems, which enables the preparation of rigidly linked conjugates containing a donor and an acceptor. The synthesis of supramolecular complexes *via* donor-acceptor bonding has certain advantages. These are the simplicity, the ability to mimic natural photosynthesis, and the possibility of controlling the strength and directionality of the interaction, resulting in efficient energy and electron transfer processes in the supramolecular system upon photoexcitation.

Impressive advances in time-resolved transient absorption, fluorescence, and EPR spectroscopy make it possible to study the dynamics of rapid processes and determine the lifetimes of charge-separated states in the systems, which is of great importance almost in all fields of science.

The introduction of various substituents into porphyrin/phthalocyanine macrocycles and fullerenes or the introduction of additional donor or acceptor ligands and the variation of the central cation (metal) enabled the synthesis of molecular systems with desired physicochemical properties. The review addresses diverse possible cations in fullerene-containing macroheterocyclic complexes. It is shown that systems containing MPorph or MPc (M = Mg, Cu, Co, Mn, Al, Sn, *etc*.) as the donor platforms are promising photoactive components, and gold porphyrin complexes can be used as acceptor components. Photovoltaic technology is one of numerous possible fields of practical application of such molecular systems. The complexes considered in the review hold promise as single-molecule magnets, compounds with liquid-crystalline properties, in nanotechnology and in the development of materials with biochemical and medical applications,[168] as agent for the targeted drug delivery, and as antibacterial/antifungal agents.

This study was financially supported by the Council on Grants at the President of the Russian Federation (Program of the state support of young Russian scientists — candidates and doctors of Sciences, Grant MK-1741.2020.3).

References

1. C. K. C. Bikram, F. D´Souza, *Coord. Chem. Rev.*, 2016, **322**, 104; DOI: 10.1016/j.ccr.2016.05.012.
2. P. A. Liddell, J. P. Sumida, A. N. Macpherson, L. Noss, G. R. Seely, K. N. Clark, A. L. Moore, T. A. Moore, D. Gust, *Photochem. Photobiol.*, 1994, **60**, 537; DOI: 10.1111/j.1751-1097.1994.tb05145.x.
3. F. D´Souza, O. Ito, *Coord. Chem. Rev.*, 2005, **249**, 1410; DOI: 10.1016/j.ccr.2005.01.002.
4. D. V. Androsov, A. A. Strelnikov, A. S. Konev, D. A. Lukyanov, A. V. Kazakova, O. V. Levin, A. F. Khlebnikov, *Russ. Chem. Bull.*, 2019, **68**, 825; DOI: 10.1007/s11172-019-2491-6.
5. O. Trukhina, M. Rudolf, G. Bottari, T. Akasaka, L. Echegoyen, T. Torres, D. M. Guldi, *J. Am. Chem. Soc.*, 2015, **137**, 12914; DOI: 10.1021/jacs.5b06454.
6. M. R. Wasielewski, *Chem. Rev.*, 1992, **92**, 435; DOI: 10.1021/cr00011a005.
7. D. Gust, T. A. Moore, A. L. Moore, *Acc. Chem. Rev.*, 1993, **26**, 198; DOI: 10.1021/ar00028a010.
8. N. V. Tkachenko, H. Lemmetyinen, in *Handbook of Carbon Nano Materials*, Eds F. D´Souza, K. M. Kadish, World Scientific Publishing Co, Singapore, 2011, Vol. **1**—**2**, p. 405—440; DOI: 10.1142/9789814327824_0013.
9. G. Bottari, O. Trukhina, M. Ince, T. Torres, *Coord. Chem. Rev.*, 2012, **256**, 2453; DOI: org/10.1016/j.ccr.2012.03.011.
10. L. J. Santos, D. CarvalhoDa-Silva, J. S. Rebouças, M. R. A. Alves, Y. M. Idemori, T. Matencio, R. P. Freitas, R. B. Alves, *Tetrahedron*, 2011, **67**, 228; DOI: 10.1016/j.tet.2010.10.066.
11. F. D´Souza, G. R. Deviprasad, M. E. Zandler, V. T. Hoang, A. Klykov, M. Van Stipdonk, A. Perera, M. E. El-Khouly, M. Fujitsuka, O. Ito, *J. Phys. Chem. A*, 2002, **106**, 3243; DOI: 10.1021/jp013165i.
12. M. V. Martínez-Díaz, N. S. Fender, M. S. Rodríguez-Morgade, M. Gómez-López, F. Diederich, L. Echegoyen, J. F. Stoddart, T. Torres, *J. Mater. Chem.*, 2002, **12**, 2095; DOI: 10.1039/B110270M.
13. P. A. Troshin, A. S. Peregudov, S. I. Troyanov, R. N. Lyubovskaya, *Russ. Chem. Bull.*, 2008, **57**, 887; DOI: 10.1007/s11172-008-0126-4.
14. S. Nayak, A. Ray, S. Bhattacharya, A. Bauri, S. Banerjee, *J. Mol. Liq.*, 2019, **290**, 110842; DOI: 10.1016/j.molliq.2019.04.119.
15. F. D´Souza, M. E. El-Khouly, S. Gadde, A. L. McCarty, P. A. Karr, M. E. Zandler, Y. Araki, O. Ito, *J. Phys. Chem. B*, 2005, **109**, 10107; DOI: 10.1021/jp0505911.
16. T. Ichiki, Y. Matsuo, E. Nakamura, *Chem. Commun.*, 2013, **49**, 279; DOI: 10.1039/C2CC36988E.
17. V. A. Basiuk, D. E. Tahuilan-Anguiano, *Chem. Phys. Lett.*, 2019, **722**, 146; DOI: 10.1016/j.cplett.2019.03.019.
18. D. Sun, F. S. Tham, C. A. Reed, L. Chaker, P. D. W. Boyd, *J. Am. Chem. Soc.*, 2002, **124**, 6604; DOI: 10.1021/ja002214m.

19. N. Zarrabi, C. Agatemor, G. N. Lim, A. J. Matula, B. J. Bayard, V. S. Batista, F. D´Souza, P. K. Poddutoori, *J. Phys. Chem. C*, 2019, **123**, 131; DOI: 10.1021/acs.jpcc.8b09500.
20. P. K. Poddutoori, A. S. D. Sandanayaka, T. Hasobe, O. Ito, A. van der Est, *J. Phys. Chem. B*, 2010, **114**, 14348; DOI: 10.1021/jp911937d.
21. A. Amati, P. Cavigli, A. Kahnt, M. T. Indelli, E. Iengo, *J. Phys. Chem. A*, 2017, **121**, 4242; DOI: 10.1021/acs.jpca.7b02973.
22. H. Zhao, Y. Zhu, C. Chen, J. Zheng, *Polymer*, 2014, **55**, 1913; DOI: 10.1016/j.polymer.2014.02.058.
23. H. J. Kim, K.-M. Park, T. K. Ahn, S. K. Kim, K. S. Kim, D. Kim, H.-J. Kim, *Chem. Commun.*, 2004, 2594; DOI: 10.1039/B411482E.
24. H. Xu, J. Zheng, *Macromol. Chem. Phys.*, 2010, **211**, 2125; DOI: 10.1002/macp.201000162.
25. E. N. Ovchenkova, N. G. Bichan, T. N. Lomova, *Russ. J. Inorg. Chem.*, 2018, **63**, 391; DOI: 10.1134/S0036023618030178.
26. T. N. Lomova, M. E. Malov, M. V. Klyuev, P. A. Troshin, *Macroheterocycles*, 2009, **2**, 164; DOI: 10.6060/mhc2009.2.164.
27. N. G. Bichan, E. N. Ovchenkova, N. O. Kudryakova, T. N. Lomova, *J. Coord. Chem.*, 2017, **70**, 2371; DOI: 10.1080/00958972.2017.1335867.
28. N. G. Bichan, E. N. Ovchenkova, N. O. Kudryakova, A. A. Ksenofontov, M. S. Gruzdev, T. N. Lomova, *New J. Chem.*, 2018, **42**, 12449; DOI: 10.1039/C8NJ00887F.
29. E. N. Ovchenkova, N. G. Bichan, N. O. Kudryakova, T. N. Lomova, *J. Mol. Liq.*, 2019, **280**, 382; DOI: 10.1016/j.molliq.2019.01.025.
30. E. N. Ovchenkova, N. G. Bichan, T. N. Lomova, *Dyes Pigm.*, 2016, **128**, 263; DOI: 10.1016/j.dyepig.2016.02.0.
31. E. N. Ovchenkova, N. G. Bichan, M. S. Gruzdev, T. N. Lomova, *Russ. J. Struct. Chem.*, 2018, **59**, 711; DOI: 10.1134/S0022476618030320.
32. N. G. Bichan, E. N. Ovchenkova, V. A. Mozgova, N. O. Kudryakova, T. N. Lomova, *Russ. J. Inorg. Chem.*, 2019, **64**, 605; DOI: 10.1134/S0036023619050024.
33. N. G. Bichan, E. N. Ovchenkova, T. N. Lomova, *Russ. J. Inorg. Chem.*, 2018, **63**, 1453; DOI: 10.1134/S0036023618110037.
34. D. V. Konarev, S. S. Khasanov, G. Saito, R. N. Lyubovskaya, *Cryst. Growth Desin.*, 2009, **9**, 1170; DOI: 10.1021/cg8010184.
35. D. V. Konarev, S. S. Khasanov, A. B. Kornev, M. A. Faraonov, P. A. Troshin, R. N. Lyubovskaya, *Dalton Trans.*, 2012, **41**, 791; DOI: 10.1039/C1DT11040C.
36. D. V. Konarev, S. S. Khasanov, M. A. Faraonov, R. N. Lyubovskaya, *CrystEngComm*, 2012, **14**, 4350; DOI: 10.1039/C2CE25295C.
37. E. V. Motorina, T. N. Lomova, M. V. Klyuev, *Mendeleev Commun.*, 2018, **28**, 426; DOI: 10.1016/j.mencom.2018.07.029.
38. E. V. Motorina, T. N. Lomova, P. A. Troshin, M. V. Klyuev, *Russ. J. Gen. Chem.*, 2014, **84**, 946.
39. T. N. Lomova, E. V. Motorina, M. V. Klyuev, *Makrogeterotsikly* [*Macroheterocycles*], 2013, **6**(4), 327 (in Russian); DOI: 10.6060/mhc130644l.
40. N. G. Bichan, E. Yu. Tyulyaeva, T. N. Lomova, A. S. Semeikin, *Russ. J. Org. Chem.*, 2014, **50**, 1361; DOI: 10.1134/S1070428014090218.
41. N. G. Bichan, E. N. Ovchenkova, T. N. Lomova, *Russ. J. Phys. Chem.*, 2019, **93**, 703; DOI: 10.1134/S004445371904006X.
42. M. S. Rodríguez-Morgade, M. E. Plonska-Brzezinska, A. J. Athans, E. Carbonell, G. de Miguel, D. M. Guldi, L. Echegoyen, T. Torres, *J. Am. Chem. Soc.*, 2009, **131**, 10484; DOI: 10.1021/ja902471w.
43. T. Da Ros, M. Prato, D. M. Guldi, M. Ruzzi, L. Pasimeni, *Chem.—Eur. J.*, 2001, **7**, 816; DOI: 10.1002/1521-3765(20010216)7:4<816::AID-CHEM816>3.0.CO;2-A.
44. T. N. Lomova, V. V. Korolev, N. G. Bichan, E. N. Ovchenkova, A. G. Ramazanova, O. V. Balmasova, M. S. Gruzdev, *Synth. Met.*, 2019, **253**, 116; DOI: 10.1016/j.synthmet.2019.05.004.
45. M. H. Moinuddin Khan, K. R. Venugopala Reddy, J. Keshavayya, *J. Coord. Chem.*, 2009, **62**, 854; DOI: 10.1080/00958970802314969.
46. N. E. Grammatikova, L. George, Z. Ahmed, N. R. Candeias, N. A. Durandin, A. Efimov, *J. Mater. Chem. B*, 2019, **7**, 4379; DOI: 10.1039/C9TB01095E.
47. E. A. Safonova, I. N. Meshkov, M. A. Polovkova, M. V. Volostnykh, A. Y. Tsivadze, Y. G. Gorbunova, *Mendeleev Commun.*, 2018, **28**, 275; DOI: 10.1016/j.mencom.2018.05.015.
48. R. Kubota, T. Takabe, K. Arima, H. Taniguchi, S. Asayama, H. Kawakami, *J. Mater. Chem. B*, 2018, **6**, 7050; DOI: 10.1039/C8TB01204K.
49. D. Kuciauskas, S. Lin, G. R. Seely, A. L. Moore, T. A. Moore, D. Gust, T. Drovetskaya, C. A. Reed, P. D. W. Boyd, *J. Phys. Chem.*, 1996, **100**, 15926; DOI: 10.1021/jp9612745.
50. T. Drovetskaya, C. A. Reed, P. Boyd, *Tetrahedron Lett.*, 1995, **36**, 7971; DOI: 10.1016/0040-4039(95)01719-X.
51. H. Imahori, K. Hagiwara, T. Akiyama, S. Taniguchi, T. Okada, Y. Sakata, *Chem. Lett.*, 1995, **24**, 265; DOI: 10.1246/cl.1995.265.
52. H. Imahori, K. Hagiwara, M. Aoki, T. Akiyama, S. Taniguchi, T. Okada, M. Shirakawa, Y. Sakata, *J. Am. Chem. Soc.*, 1996, **118**, 11771; DOI: 10.1021/ja9628415.
53. M. Prato, M. Maggini, C. Giacometti, G. Scorrano, G. Sandona, G. Farnia, *Tetrahedron*, 1996, **52**, 5221; DOI: 10.1016/0040-4020(96)00126-3.
54. G. Zheng, T. J. Dougherty, R. K. Pandey, *Chem. Commun.*, 1999, 2469; DOI: 10.1039/A906889I.
55. G. Li, M. P. Dobhal, M. Shibata, R. K. Pandey, *Org. Lett.*, 2004, **6**, 2393; DOI: 10.1021/ol0492290.
56. K. Ohkubo, H. Kotani, J. Shao, Z. Ou, K. M. Kadish, G. Li, R. K. Pandey, M. Fujitsuka, O. Ito, H. Imahori, S. Fukuzumi, *Angew. Chem., Int. Ed.*, 2004, **43**, 853; DOI: 10.1002/anie.200352870.
57. R. K. Pandey, L. N. Goswami, Y. Chen, A. Gryshuk, J. R. Missert, A. Oseroff, T. J. Dougherty, *Lasers Surg. Med.*, 2006, **38**, 445; DOI: 10.1002/lsm.20352.
58. A. F. Mironov, *Macroheterocycles*, 2011, **4**, 186; DOI: 10.6060/mhc2011.3.08.
59. T. D. M. Bell, T. A. Smith, K. P. Ghiggino, M. G. Ranasinghe, M. J. Shephard, M. N. Paddon-Row, *Chem. Phys. Lett.*, 1997, **268**, 223; DOI: 10.1016/S0009-2614(97)00193-0.
60. M. Wedel, F.-P. Montforts, *Tetrahedron Lett.*, 1999, **40**, 7071; DOI: 10.1016/S0040-4039(99)01471-9.
61. A. Graja, I. Olejniczak, A. Bogucki, D. Bonifazi, F. Diederich, *Chem. Phys.*, 2004, **300**, 227; DOI: 10.1016/j.chemphys.2004.02.005.
62. V. Vehmanen, N. V. Tkachenko, H. Imahori, S. Fukuzumi, H. Lemmetyinen, *Spectrochim. Acta, Part A*, 2001, **57**, 2229; DOI: 10.1016/s1386-1425(01)00496-6.
63. M. A. Fazio, O. P. Lee, D. I. Schuster, *Org. Lett.*, 2008, **10**, 4979; DOI: 10.1021/ol802053k.
64. D. Sukeguchi, H. Yoshiyama, N. Shibata, S. Nakamura, T. Toru, Y. Hayashi, T. Soga, *J. Fluorine Chem.*, 2009, **130**, 361; DOI: 10.1016/j.jfluchem.2008.11.005.

65. E. S. Zyablikova, N. A. Bragina, A. F. Mironov, *Mendeleev Commun.*, 2012, **22**, 257; DOI: 10.1016/j.mencom.2012.09.010.
66. C. Solis, M. B. Ballatore, M. B. Suarez, M. E. Milanesio, E. N. Durantini, M. Santo, T. Dittrich, L. Otero, M. Gervaldo, *Electrochim. Acta*, 2017, **238**, 81; DOI: 10.1016/j.electacta.2017.04.015.
67. Z.-Y. Wu, S.-Y. Yang, *J. Mol. Struct.*, 2019, **1188**, 244; DOI: 10.1016/j.molstruc.2019.04.013.
68. E. S. Krutikova, N. A. Bragina, A. F. Mironov, *Macroheterocycles*, 2011, **4**, 130; DOI: 10.6060/mhc2011.2.13.
69. K. Lewandowska, K. Szaciłowski, *Aust. J. Chem.*, 2011, **64**, 1409; DOI: 10.1071/CH11051.
70. M. Lederer, M. Ince, M. V. Martinez-Diaz, T. Torres, D. M. Guldi, *ChemPlusChem*, 2016, **81**, 941; DOI: 10.1002/cplu.201600197.
71. M. Quintiliani, A. Kahnt, T. Wölfle, W. Hieringer, P. Vázquez, A. Görling, D. M. Guldi, T. Torres, *Chem.—Eur. J.*, 2008, **14**, 3765; DOI: 10.1002/chem.200701700.
72. A. I. Kotel´nikov, A. Y. Rybkin, N. S. Goryachev, A. Y. Belik, A. B. Kornev, P. A. Troshin, *Dokl. Phys. Chem.*, 2013, **452**, 229 DOI: 10.1134/S0012501613080046.
73. A. Yu. Belik, P. A. Mikhailov, O. A. Kraevaya, A. Yu. Rybkin, E. A. Khakina, N. S. Goryachev, L. I. Usoltseva, Yu. V. Romanenko, O. I. Koifman, O. I. Gushchina, A. F. Mironov, P. A. Troshin, A. I. Kotel´nikov, *Dokl. Phys. Chem.*, 2017, **477**, 222 DOI: 10.1134/S0012501617120065.
74. A. Y. Rybkin, A. Y. Belik, N. S. Goryachev, P. A. Mikhaylov, O. A. Kraevaya, N. V. Filatova, I. I. Parkhomenko, A. S. Peregudov, A. A. Terent´ev, E. A. Larkina, A. F. Mironov, P. A. Troshin, A. I. Kotelnikov, *Dyes Pigm.*, 2020, **180**, 108411; DOI: 10.1016/j.dyepig.2020.108411.
75. R. C. Dougherty, H. H. Strain, W. A. Svec, R. A. Uphaus, J. J. Katz, *J. Am. Chem. Soc.*, 1966, **88**, 5037; DOI: 10.1021/ja00712a037.
76. M. E. El-Khouly, Y. Araki, O. Ito, S. Gadde, A. L. McCarty, P. A. Karr, M. E. Zandler, F. D´Souza, *Phys. Chem. Chem. Phys.*, 2005, **7**, 3163; DOI: 10.1039/B507673K.
77. F. D´Souza, S. Gadde, M. E. Zandler, K. Arkady, M. E. El-Khouly, M. Fujitsuka, O. Ito, *J. Phys. Chem. A*, 2002, **106**, 12393; DOI: 10.1021/jp021926r.
78. T. Arlt, S. Schmidt, W. Kaiser, C. Lauterwasser, M. Meyer, H. Scheer, W. Zinth, *Proc. Nat. Acad. Sci.*, 1993, **90**, 11757; DOI: 10.1073/pnas.90.24.11757.
79. P. Prashanth Kumar, B. G. Maiya, *New J. Chem.*, 2003, **27**, 619; DOI: 10.1039/B208339F.
80. P. K. Poddutoori, A. S. D. Sandanayaka, N. Zarrabi, T. Hasobe, O. Ito, A. van der Est, *J. Phys. Chem. A*, 2011, **115**, 709; DOI: 10.1021/jp110156w.
81. P. K. Poddutoori, G. N. Lim, A. S. D. Sandanayaka, P. A. Karr, O. Ito, F. D´Souza, M. Pilkington, A. van der Est, *Nanoscale*, 2015, **7**, 12151; DOI: 10.1039/C5NR01675D.
82. Z. Yu, H. Tian, E. Gabrielsson, G. Boschloo, M. Gorlov, L. Sun, L. Kloo, *RSC Adv.*, 2012, **2**, 1083; DOI: 10.1039/C1RA00877C.
83. S. Wenger, P.-A. Bouit, Q. Chen, J. Teuscher, D. D. Censo, R. Humphry-Baker, J.-E. Moser, J. L. Delgado, N. Martín, S. M. Zakeeruddin, M. Grätzel, *J. Am. Chem. Soc.*, 2010, **132**, 5164; DOI: 10.1021/ja909291h.
84. Q. Chen, X. Li, T. Jiu, S. Ma, J. Li, X. Xiao, W. Zhang, *Dyes Pigm.*, 2017, **147**, 113; DOI: 10.1016/j.dyepig.2017.08.007.
85. D. P. Arnold, J. Blok, *Coord. Chem. Rev.*, 2004, **248**, 299; DOI: 10.1016/j.ccr.2004.01.004.
86. M. E. El-Khouly, E. S. Kang, K.-Y. Kay, C. S. Choi, Y. Aaraki, O. Ito, *Chem.—Eur. J.*, 2007, **13**, 2854; DOI: 10.1002/chem.200601254.
87. L. Martín-Gomis, K. Ohkubo, F. Fernández-Lázaro, S. Fukuzumi, Á. Sastre-Santos, *Org. Lett.*, 2007, **9**, 3441; DOI: 10.1021/ol701444d.
88. M. E. El-Khouly, J. H. Kim, K.-Y. Kay, C. S. Choi, O. Ito, S. Fukuzumi, *Chem.—Eur. J.*, 2009, **15**, 5301; DOI: 10.1002/chem.200900165.
89. L. Martín-Gomis, K. Ohkubo, F. Fernández-Lázaro, S. Fukuzumi, Á. Sastre-Santos, *Chem. Commun.*, 2010, **46**, 3944; DOI: 10.1039/C002077J.
90. M. E. El-Khouly, J.-H. Kim, K.-Y. Kay, S. Fukuzumi, *J. Porphyrins Phthalloc.*, 2013, **17**, 1055; DOI: 10.1142/S1088424613501046.
91. L. Martín-Gomis, S. Seetharaman, P. Karr, F. Fernández Lázaro, F. D´Souza, A. Sastre-Santos, *Chem.—Eur. J.*, 2020, **26**, 4822; DOI: 10.1002/chem.201905605.
92. L. Martín-Gomis, F. Peralta-Ruiz, M. B. Thomas, F. Fernández-Lázaro, F. D´Souza, Á. Sastre-Santos, *Chem.—Eur. J.*, 2017, **23**, 3863; DOI: 10.1002/chem.201603741.
93. K. Ishikawa, A. Watarai, M. Yasutake, K. Ohta, *J. Porphyr. Phthaloc.*, 2018, **22**, 693; DOI: 10.1142/S108842461850092X.
94. H. Murakami, R. Matsumoto, Y. Okusa, T. Sagara, M. Fujitsuka, O. Ito, N. Nakashima, *J. Mater. Chem.*, 2002, **12**, 2026; DOI: 10.1039/B201145J.
95. T. G. Linssen, K. Dürr, M. Hanack, A. Hirsch, *J. Chem. Soc., Chem. Commun.*, 1995, 103; DOI: 10.1039/C39950000103.
96. A. S. Shalabi, S. Abdel Aal, A. M. El Mahdy, *Mol. Simul.*, 2013, **39**, 689; DOI: 10.1080/08927022.2012.758853.
97. C. O. Obondi, G. N. Lim, F. D´Souza, *J. Phys. Chem. C*, 2015, **119**, 176; DOI: 10.1021/jp511310c.
98. C. O. Obondi, G. N. Lim, B. Churchill, P. K. Poddutoori, A. van der Est, F. D´Souza, *Nanoscale*, 2016, **8**, 8333; DOI: 10.1039/C6NR01083K.
99. S. Shetab-Boushehri, S. Ostad, S. Sarkar, D. Kuznetsov, A. Buchachenko, M. Orlova, B. Minaii, A. Kebriaeezadeh, M. Rezayat, *Acta Med. Iranica*, 2010, **48**, 342.
100. M. B. Spesia, M. E. Milanesio, E. N. Durantini, *Eur. J. Med. Chem.*, 2008, **43**, 853; DOI: 10.1016/j.ejmech.2007.06.014.
101. M. Wang, S. Maragani, L. Huang, S. Jeon, T. Canteenwala, M. R. Hamblin, L. Y. Chiang, *Eur. J. Med. Chem.*, 2013, **63**, 170; DOI: 10.1016/j.ejmech.2013.01.052.
102. R. Yin, M. Wang, Y.-Y. Huang, G. Landi, D. Vecchio, L. Y. Chiang, M. R. Hamblin, *Free Radical Biol. Med.*, 2015, **79**, 14; DOI: 10.1016/j.freeradbiomed.2014.10.514.
103. S. H. Friedman, D. L. DeCamp, R. P. Sijbesma, G. Srdanov, F. Wudl, G. L. Kenyon, *J. Am. Chem. Soc.*, 1993, **115**, 6506; DOI: 10.1021/ja00068a005.
104. N. E. Fedorova, R. R. Klimova, Y. A. Tulenev, E. V. Chichev, A. B. Kornev, P. A. Troshin, A. A. Kushch, *Mendeleev Commun.*, 2012, **22**, 254; DOI: 10.1016/j.mencom.2012.09.009.
105. L. Tauchi, T. Nakagaki, M. Shimizu, E. Itoh, M. Yasutake, K. Ohta, *J. Porphyrins Phthaloc.*, 2013, **17**, 1080; DOI: 10.1142/S1088424613500752.
106. M. Shimizu, L. Tauchi, T. Nakagaki, A. Ishikawa, E. Itoh, K. Ohta, *J. Porphyrins Phthaloc.*, 2013, **17**, 264; DOI: 10.1142/S1088424613500168.
107. A. Ishikawa, K. Ono, K. Ohta, M. Yasutake, M. Ichikawa, E. Itoh, *J. Porphyrins Phthaloc.*, 2014, **18**, 366; DOI: 10.1142/S1088424614500072.

108. Y. Han, L. Chen, Y. Chen, *J. Polym. Sci., Part A: Polym. Chem.*, 2013, **51**, 258; DOI: 10.1002/pola.26394.
109. O. Thiebaut, H. Bock, E. Grelet, *J. Am. Chem. Soc.* 2010, **132**, 6886; DOI: 10.1021/ja1012596.
110. C. Bingel, *Chem. Ber.*, 1993, **126**, 1957; DOI: 10.1002/cber.19931260829.
111. T. Kamei, T. Kato, E. Itoh, K. Ohta, *J. Porphyrins Phthaloc.*, 2012, **16**, 1261; DOI: 10.1142/S1088424612501349.
112. P. K. Poddutoori, Y. E. Kandrashkin, C. O. Obondi, F. D´Souza, A. van der Est, *Phys. Chem. Chem. Phys.*, 2018, **20**, 28223; DOI: 10.1039/C8CP04937H.
113. M. Ince, A. Hausmann, M. V. Martinez-Diaz, D. M. Guldi, T. Torres, *Chem. Commun.*, 2012, **48**, 4058; DOI: 10.1039/C2CC30632H.
114. T. Torres, A. Gouloumis, D. Sanchez-Garcia, J. Jayawickramarajah, W. Seitz, D. M. Guldi, J. L. Sessler, *Chem. Commun.*, 2007, 292; DOI: 10.1039/B613086K.
115. J. L. Sessler, J. Jayawickramarajah, A. Gouloumis, T. Torres, D. M. Guldi, S. Maldonado, K. J. Stevenson, *Chem. Commun.*, 2005, 1892; DOI: 10.1039/B418345B.
116. D. M. Guldi, J. Ramey, M. V. Martínez-Díaz, A. d. l. Escosura, T. Torres, T. Da Ros, M. Prato, *Chem. Commun.* 2002, 2774; DOI: 10.1039/B208516J.
117. A. S. D. Sandanayaka, Y. Araki, O. Ito, R. Chitta, S. Gadde, F. D´Souza, *Chem. Commun.*, 2006, 4327; DOI: 10.1039/B610171B.
118. L. Basurto, F. Amerikheirabadi, R. Zope, T. Baruah, *Phys. Chem. Chem. Phys.*, 2015, **17**, 5832; DOI: 10.1039/C4CP04583A.
119. T. Nojiri, M. M. Alam, H. Konami, A. Watanabe, O. Ito, *J. Phys. Chem. A*, 1997, **101**, 7943; DOI: 10.1021/jp9714734.
120. D. V. Konarev, S. S. Khasanov, A. Otsuka, G. Saito, R. N. Lyubovskaya, *Inorg. Chem.*, 2007, **46**, 2261; DOI: 10.1021/ic0611138.
121. D. V. Konarev, S. S. Khasanov, Y. L. Slovokhotov, G. Saito, R. N. Lyubovskaya, *CrystEngComm*, 2008, **10**, 48; DOI: 10.1039/B708100F.
122. F. D´Souza, G. R. Deviprasad, M. S. Rahman, J.-p. Choi, *Inorg. Chem.*, 1999, **38**, 2157; DOI: 10.1021/ic981358n.
123. M. E. El-Khouly, L. M. Rogers, M. E. Zandler, G. Suresh, M. Fujitsuka, O. Ito, F. D´Souza, *ChemPhysChem*, 2003, **4**, 474; DOI: 10.1002/cphc.200200540.
124. A. N. Lapshin, V. A. Smirnov, R. N. Lyubovskaya, N. F. Goldshleger, *Russ. Chem. Bull.*, 2005, **54**, 2338; DOI: 10.1007/s11172-006-0119-0.
125. I. A. Mochalov, A. N. Lapshin, V. A. Nadtochenko, V. A. Smirnov, N. F. Goldshleger, *Russ. Chem. Bull.*, 2006, **55**, 1598; DOI: 10.1007/s11172-006-0460-3.
126. M. M. Olmstead, D. A. Costa, K. Maitra, B. C. Noll, S. L. Phillips, P. M. Van Calcar, A. L. Balch, *J. Am. Chem. Soc.*, 1999, **121**, 7090; DOI: 10.1021/ja990618c.
127. E. I. Yudanova, D. V. Konarev, L. L. Gumanov, R. N. Lyubovskaya, *Russ. Chem. Bull.*, 1999, **48**, 718; DOI: 10.1007/BF02496254.
128. D. V. Konarev, I. S. Neretin, Y. L. Slovokhotov, E. I. Yudanova, N. V. Drichko, Y. M. Shul´ga, B. P. Tarasov, L. L. Gumanov, A. S. Batsanov, J. A. K. Howard, R. N. Lyubovskaya, *Chem.—Eur. J.*, 2001, **7**, 2605; DOI: 10.1002/15213765(20010618)7:12<2605::AID-CHEM26050>3.0.CO;2-P.
129. D. V. Konarev, S. S. Khasanov, A. Otsuka, Y. Yoshida, G. Saito, *Synth. Met.*, 2003, **133—134**, 707; DOI: 10.1016/S0379-6779(02)00426-5.
130. D. V. Konarev, S. S. Khasanov, G. Saito, R. N. Lyubovskaya, Y. Yoshida, A. Otsuka, *Chem.—Eur. J.*, 2003, **9**, 3837; DOI: 10.1002/chem.200204470.
131. T. Ishii, R. Kanehama, N. Aizawa, M. Yamashita, H. Matsuzaka, K. I. Sugiura, H. Miyasaka, T. Koda ma, K. Kikuchi, I. Ikemoto, H. Tanaka, K. Marumoto, S. I. Kuroda, J. Chem. Soc., Dalton Trans., 2001, 2975; DOI: 10.1039/B104514H.
132. D. V. Konarev, S. S. Khasanov, R. N. Lyubovskaya, *Coord. Chem. Rev.*, 2014, **262**, 16; DOI: 10.1016/j.ccr.2013.10.021.
133. D. M. Guldi, *Chem. Commun.*, 2000, 321; DOI: 10.1039/A907807J.
134. K. M. Kadish, L. R. Shiue, *Inorg. Chem.*, 1982, **21**, 1112; DOI: 10.1021/ic00133a046.
135. G. A. Metselaar, J. K. M. Sanders, J. de Mendoza, *Dalton Trans.*, 2008, 588; DOI: 10.1039/B717017N.
136. P. K. Poddutoori, P. Poddutoori, B. G. Maiya, T. K. Prasad, Y. E. Kandrashkin, S. Vasil´ev, D. Bruce, A. van der Est, *Inorg. Chem.*, 2008, **47**, 7512; DOI: 10.1021/ic702480m.
137. A. Bagaki, H. B. Gobeze, G. Charalambidis, A. Charisiadis, C. Stangel, V. Nikolaou, A. Stergiou, N. Tagmatarchis, F. D´Souza, A. G. Coutsolelos, *Inorg. Chem.*, 2017, **56**, 10268; DOI: 10.1021/acs.inorgchem.7b01050.
138. N. Zarrabi, C. O. Obondi, G. N. Lim, S. Seetharaman, B. G. Boe, F. D´Souza, P. K. Poddutoori, *Nanoscale*, 2018, **10**, 20723; DOI: 10.1039/C8NR06649C.
139. A. R. Da Silva, A. C. Pelegrino, A. C. Tedesco, R. A. Jorge, *J. Braz. Chem. Soc.*, 2008, **19**, 491; DOI: 10.1590/S0103-50532008000300017.
140. P. Dechan, G. D. Bajju, *J. Mol. Struct.*, 2019, **1195**, 140; DOI: 10.1016/j.molstruc.2019.05.120.
141. S. G. Ang, H. G. Ang, W. Han, B. W. Sun, M. K. Y. Lee, Y. W. Lee, G. Y. Yang, *Proceedings of SPIEV,* 2002, **4798**, 195; DOI: 10.1117/12.451927.
142. G. Y. Yang, S. G. Ang, L. L. Chng, Y. W. Lee, E. W.-P. Lau, K. S. Lai, H. G. Ang, *Chem.—Eur. J.*, 2003, **9**, 900; DOI: 10.1002/chem.200390111.
143. T. N. Lomova, M. E. Malov, M. V. Klyuev, P. A. Troshin, *Reactions of the Pyridine Substituted N-Metylpyrrolidinil[60]-fullerene-(5,10,15,20-tetraphenylporphyrinato)(chloro)-Indium(III) Diade Formation*, Nova Science Publishers, New York, 2010, p. 143.
144. T. Da Ros, M. Prato, M. Carano, P. Ceroni, F. Paolucci, S. Roffia, L. Valli, D. Guldi, *J. Organomet. Chem.*, 2000, **599**, 62; DOI: 10.1016/S0022-328X(99)00754-8.
145. A. Mateo-Alonso, C. Ehli, D. M. Guldi, M. Prato, *J. Am. Chem. Soc.*, 2008, **130**, 14938; DOI: 10.1021/ja8063155.
146. N. G. Bichan, E. N. Ovchenkova, V. A. Mozgova, N. O. Kudryakova, M. S. Gruzdev, T. N. Lomova, *Russ. J. Phys. Chem.*, 2020, **94**, 1159; DOI: 10.1134/S003602442006006.
147. E. N. Ovchenkova, N. G. Bichan, A. A. Tsaturyan, N. O. Kudryakova, M. S. Gruzdev, F. E. Gostev, I. V. Shelaev, V. A. Nadtochenko, T. N. Lomova, *J. Phys. Chem. C*, 2020, **124**, 4010; DOI: 10.1021/acs.jpcc.9b11661.
148. E. N. Ovchenkova, N. G. Bichan, T. N. Lomova, *Russ. J. Org. Chem.*, 2016, **52**, 1503; DOI: 10.1134/S1070428016100213.
149. E. N. Ovchenkova, N. G. Bichan, T. N. Lomova, *Tetrahedron*, 2015, **71**, 6659; DOI: 10.1016/j.tet.2015.07.054.
150. E. N. Ovchenkova, N. G. Bichan, N. O. Kudryakova, A. A. Ksenofontov, T. N. Lomova, *Dyes Pigm.*, 2018, **153**, 225; DOI: 10.1016/j.dyepig.2018.02.023.

151. E. N. Ovchenkova, N. G. Bichan, T. N. Lomova, *Russ. J. Phys. Chem.*, 2019, **93**, 62; DOI: 10.1134/S0036024419010217.
152. E. N. Ovchenkova, N. G. Bichan, A. A. Ksenofontov, T. N. Lomova, *J. Fluorine Chem.*, 2019, **224**, 113; DOI: 10.1016/j.jfluchem.2019.06.002.
153. E. V. Motorina, T. N. Lomova, E. G. Mozhzhukhina, M. S. Gruzdev, *Russ. J. Inorg. Chem.*, 2019, **64,** 1538; DOI: 10.1134/S0036023619120106.
154. S. K. Das, B. Song, A. Mahler, V. N. Nesterov, A. K. Wilson, O. Ito, F. D´Souza, *J. Phys. Chem. C*, 2014, **118**, 3994; DOI: 10.1021/jp4118166.
155. C. K. C. Bikram, N. K. Subbaiyan, F. D´Souza, *J. Phys. Chem. C*, 2012, **116**, 11964; DOI: 10.1021/jp303227s.
156. S. K. Das, A. Mahler, A. K. Wilson, F. D´Souza, *ChemPhysChem*, 2014, **15**, 2462; DOI: 10.1002/cphc.201402118.
157. A. Harriman, V. Heitz, J. P. Sauvage, *J. Phys. Chem.*, 1993, **97**, 5940; DOI: 10.1021/j100124a027.
158. A. M. Brun, A. Harriman, V. Heitz, J. P. Sauvage, *J. Am. Chem. Soc.*, 1991, **113**, 8657; DOI: 10.1021/ja00023a.
159. K. Kilså, J. Kajanus, A. N. Macpherson, J. Mårtensson, B. Albinsson, *J. Am. Chem. Soc.*, 2001, **123**, 3069; DOI: 10.1021/ja003820k.
160. J. Andréasson, G. Kodis, T. Ljungdahl, A. L. Moore, T. A. Moore, D. Gust, J. Mårtensson, B. Albinsson, *J. Phys. Chem. A*, 2003, **107**, 8825; DOI: 10.1021/jp034120f.
161. J. Fortage, J. Boixel, E. Blart, L. Hammarström, H. C. Becker, F. Odobel, *Chem.—Eur. J.*, 2008, **14**, 3467; DOI: 10.1002/chem.200701335.
162. S. Fukuzumi, K. Ohkubo, W. E, Z. Ou, J. Shao, K. M. Kadish, J. A. Hutchison, K. P. Ghiggino, P. J. Sintic, M. J. Crossley, *J. Am. Chem. Soc.*, 2003, **125**, 14984; DOI: 10.1021/ja037214b.
163. K. Sonogashira, Y. Tohda, N. Hagihara, *Tetrahedron Lett.*, 1975, **16**, 4467; DOI: 10.1016/ S0040-4039(00)91094-3.
164. J. Fortage, A. Scarpaci, L. Viau, Y. Pellegrin, E. Blart, M. Falkenström, L. Hammarström, I. Asselberghs, R. Kellens, W. Libaers, K. Clays, M. P. Eng, F. Odobel, *Chem.—Eur. J.*, 2009, **15**, 9058; DOI: 10.1002/chem.200900262.
165. P. K. Poddutoori, G. N. Lim, S. Vassiliev, F. D´Souza, *Phys. Chem. Chem. Phys.*, 2015, **17**, 26346; DOI: 10.1039/C5CP04818D.
166. A. Takai, C. P. Gros, J.-M. Barbe, S. Fukuzumi, *Phys. Chem. Chem. Phys.*, 2010, **12**, 12160; DOI: 10.1039/c0cp00329h.
167. M. E. El-Khouly, S. Fukuzumi, *Photochem. Photobiol. Sci.*, 2016, **15**, 1340; DOI: 10.1039/C6PP00228E.
168. N. F. Goldshleger, M. A. Lapshina, V. E. Baulin, A. A. Shiryaev, Yu. G. Gorbunova, A. Yu. Tsivadze, *Russ. Chem. Bull.*, 2020, **69**, 1223.

Received April 24, 2020;
in revised form August 19, 2020;
accepted September 24, 2020